to be the most predictive in distinguishing between early stage NSCLC (Fig. 1(a-b)) recurrence from non-recurrence patients. A random forest classifier trained with Haralick and shape features yielded a 0.78 AUC on YTMA140, using 2/3 for training and 1/3 for validation over 100 repeated random sub-sampling and (Fig. 1(e)) 0.71 on YTMA79. Survival predictions for these 2 groups of patients was shown to be statistically different with p-value 0.02 (Fig. 1(f)).

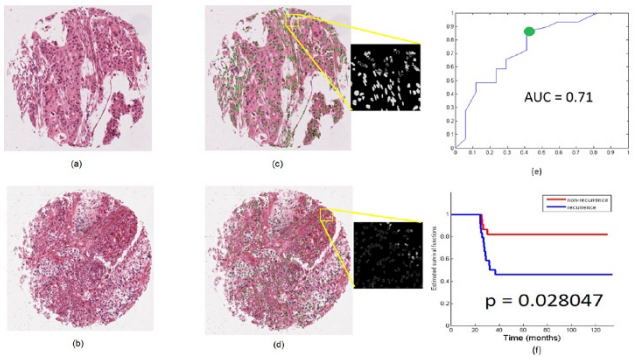

Figure 1: Sample TMA of (a) non-recurrence and (b) recurrence NSCLC. Haralick texture (standard deviation intensity correlation) feature of nuclei on (c) non-recurrence and (d) recurrence NSCLC show obvious intensity difference. (e) Receiver operating characteristic plot with operating point highlighted and (f) Kaplan-Meier curves generated via the random forest classifier.

Conclusions: We found that a combination of computer extracted nuclear texture and shape features could potentially be used to identify recurrence in early stage NSCLC. These features were found to yield a statistically significant difference in likelihood of recurrence between patients in both training and independent validation cohorts.

1584 Central Histopathology Review of Essential Thrombocythemia and Polycythemia Vera Bone Marrow Biopsies via Digital Tools in a Clinical Trial on Pegylated Interferon Alfa-2a

Delu Zhou, Olga Pozdnyakova, Rajan Dewar, Robert P Hasserjian, Ali Etman, Ronald Hoffman, Mohamed E Salama. University of Utah, Salt Lake City, UT; Brigham and Women's Hospital, Boston, MA; University of Michigan, Ann Arbor, MI; Massachusetts General Hospital, Boston, MA; Mount Sinai School of Medicine, New York, NY.

Background: Central pathology review for clinical trials often require specimen examination by pathologists from geographically separated institutions. This study is designed to explore the possibility of utilizing whole slide digital imaging (WSI) and computer-assisted image technology (CAI) to facilitate the central review process in a clinical study of polycythemia vera (PV) and essential thrombocythemia (ET) sponsored by MPD Research Consortium (MPD-RC). We report here interval pathology review findings.

Design: Cases of PV and ET patients treated with Pegylated Interferon Alfa-2a from MPD-RC clinical trial were studied. The bone marrow (BM) core biopsy H&E and reticulin slides from samples collected before and after treatment were scanned with Aperio AT-2 scanner. E-slide management system was used to provide remote access to images. Cytonuclear algorithm of HALO imaging software was used to quantify bone/hematopoietic area and cellularity. 55 samples were reviewed by at least two hematopathologists from separate institutions according to predefined criteria. 95 specimens were evaluated by CAI.

Results: Pathologists were able to successfully perform morphological evaluation via digitalized central review process. The analysis showed high agreement rate on megakaryocyte size (94%) and clustering (72%), osteosclerosis score (88%), fibrosis score (74%) , cellularity (81%) and lymphoid aggregates (88%), but low agreement for megakaryocytes nuclear lobulation (36%) and dysplasia (40%) and erythroid quantification (40%). 5/6 patients showed significant decrease in trabecular bone areaas associated with increase in fat at 24 months post-treatmentas. CAI also showed higher correlation with the average cellularity identified by direct visualization (correlation coefficient is 0.88), when compared to interobserver correlation of visual cellularity estimated by different pathologists (correlation coefficient is 0.81). PV cases showed higher cellularity relative to ET cases at baseline (p=0.0043) or post-treatment samples (p=0.029).

Conclusions: WSI is a feasible and useful tool for central pathology review in clinical trials. CAI provided added value to morphology for more objective evaluation of BM histology. High concordance can be achieved with defined criteria for histotopography evaluation.

Kidney/Renal Pathology (including Transplantation)

1585 mRNA Diagnosis of Antibody-Mediated Rejection from Routine Paraffin Sections of Renal Transplant Biopsies in a Nonhuman Primate Model

Benjamin Adam, R Neal Smith, Tatsuo Kawai, A Benedict Cosimi, Robert B Colvin, Michael Mengel. University of Alberta, Edmonton, AB, Canada; Harvard Medical School and Massachusetts General Hospital, Boston, MA.

Background: In 2013, the Banff classification proposed molecular diagnostics as an adjunct for the diagnosis of antibody-mediated rejection (ABMR) in renal allografts. To catalyze clinical adoption of this approach, we tested whether mRNA from formalin-fixed paraffin-embedded (FFPE) tissue samples could be analyzed with the new NanoString nCounter gene expression platform, using archival tissue blocks from serial protocol biopsies of nonhuman primates that developed chronic ABMR.

Design: 34 genes (endothelial, NK cell, inflammatory) previously associated with ABMR in humans were compiled into a monkey specific NanoString nCounter probe set. RNA was isolated from 56 FFPE sections (3 x 20 µm) including 48 sequential renal allograft biopsies from 12 Cynomolgus monkeys that developed ABMR after tolerance induction protocols without specific ABMR treatment (Smith et al Am J Transplant 8:1662, 2008) and compared with 8 normal kidney controls. Gene set expression was quantified and correlated with histology, C4d, and serology.

Results: Gene set expression was significantly higher in biopsies with histologic diagnoses of ABMR compared with normal controls (p=0.00007). It was also higher in C4d positive vs. negative (p=0.000007) and donor specific antibody (DSA) positive vs. negative (p=0.0006) biopsies. Some animals (e.g. 5198, 6000) exhibited increasing gene set expression with histologic ABMR progression. Other animals (e.g. 1902, 6007) demonstrated stable or decreasing expression with histologically persisting ABMR. Biopsies with histologic diagnoses of TCMR showed increased ABMR gene set expression before developing histologic evidence of ABMR, suggesting that molecular testing is predictive and more sensitive than histology for early ABMR.

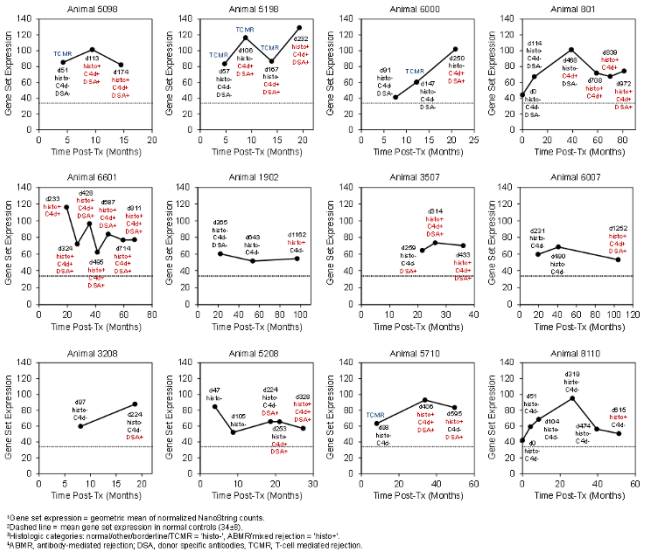

[1]Gene set expression = geometric mean of normalized NanoString counts.
[2]Dashed line = mean gene set expression in normal controls (24-52).
[3]Histologic categories: normal/other/borderline/TCMR = 'histo-'; ABMR/mixed rejection = 'histo+'.
[4]ABMR, antibody-mediated rejection; DSA, donor specific antibodies, TCMR, T-cell mediated rejection.

Conclusions: Robust multiplexed gene expression quantification from nonhuman primate FFPE renal allograft biopsies is feasible using the NanoString platform. Preliminary animal model validation indicates significant potential for a set of endothelial, NK cell, and inflammatory transcripts in diagnosing ABMR and assessing disease activity.

1586 Acute Allograft Glomerulopathy: A Distinct Form of Cellular Rejection

Osamah AL-Badri, Mariam P Alexander, Fernando G Cosio, Lynn D Cornell. Mayo Clinic, Rochester, MN.

Background: Acute allograft glomerulopathy (AAG) is a glomerular lesion of renal allografts characterized by endocapillary hypercellularity with mononuclear cell infiltration and markedly enlarged endothelial cells occluding the capillary lumen, and absence of immune complex deposits. AAG is not currently a rejection lesion recognized by the Banff schema.

Design: We searched a database for biopsies that showed AAG. Light microscopy slides and C4d staining status were reviewed, as were follow-up biopsies. Treatment and clinical follow up data were obtained.

Results: We identified 15 patients with AAG in renal allograft biopsies from Jan 2009 through Aug 2015, accounting for <1% of biopsies showing rejection during this time period. The mean patient age was 56.4 years (range 22-76); ~54% of transplants were from living donors. The mean time post-transplant was 3.2 months (range 0.1 to 11). The biopsy indication in 14 was increased serum creatinine (SCr), mean 3.2 mg/dl (range 1.5-9.4); one was a 4 month protocol biopsy.

All biopsies showed glomerulitis by definition. In addition, the glomeruli showed focal segmental to global marked endothelial enlargement with occlusion of the capillary lumens and infiltrating mononuclear cells and neutrophils. No GBM duplication was present. 12/15 (80%) showed arteritis (Banff v lesions), including 4 with v2 or v3 lesions. 8/15 (53%) showed mild or no interstitial inflammation; 9/15 (60%) showed mild or no tubulitis. 14/15 (93%) were C4d negative; one showed focal C4d PTC staining. 2 showed moderate peritubular capillaritis. 3/15 (20%) showed focal thrombi in vessels or mesangiolysis. Immunofluorescence was negative for immune complexes in all.

6/12 (50%) of patients with data available had a history of donor-specific antibody. 9 patients were on triple immunosuppression. Treatment information was available in 10 patients; all were treated with immunosuppression (anti-thymocyte globulin in 5 and steroid bolus in 5). Up to 1 year after the biopsy showing AAG, the SCr decreased in 9/13 (69%) patients alive with data available, mean 1.7 mg/dl (range 0.9-3.3). Follow up biopsies were performed in 7 patients; 5 of these (71%) showed continued AAG lesions.

Conclusions: AAG is a rare but distinct histopathologic lesion that is highly correlated with vascular rejection and rarely accompanied

by lesions associated with alloantibody. AAG should be considered a manifestation of cellular rejection of the glomerulus, possibly by a mechanism similar to endarteritis.

1587 The Pathologic Spectrum of Acute Myoglobulinuric Renal Failure

Firas Al-Delfi, Elba A Turbat-Herrera, Guillermo A Herrera. Louisiana State University Health Sciences Center in Shreveport, Shreveport, LA.

Background: Myoglobinuria can cause acute kidney injury, i.e. acute myoglobulinuric renal failure (AMGURF). The most accepted mechanism is the formation of distal nephron casts containing myoglobin. However, it is also suspected that myoglobin can be associated with proximal tubular toxicity which causes AMGURF. Only few reports in the literature exist regarding the findings in this condition. The purpose of this study is to better understand the pathogenesis of this disorder and to define diagnostic criteria at the light microscopic and ultrastructural levels for this entity.

Design: Out of 3367 kidney biopsies evaluated at our institution that were searched, 17 cases of AMGURF were identified. The clinical and pathologic findings were scrutinized in an effort to define the entire spectrum of pathologic findings in this condition. All cases were examined using H&E, usual battery of immunofluorescence stains (IgG, IgM, IgA, C3, C1q, kappa and lambda light chains, fibrinogen and albumin), myoglobin stain, and tubular damage /repair immunohistochemical markers (Kim 1, bcl 2, CD133, Ki-67 and p53) and examined ultrastructurally.

Results: In 12 out of 17 cases, rhabdomyolysis was diagnosed or suggested via clinical and/or laboratory findings. Out of these 12 cases, 4 were associated with a viral infection and 2 were illicit-drugs related. The pathology observed in all cases was in the tubulointerstitial compartment, including proximal tubular damage, interstitial edema, focal and generally mild interstitial inflammation invariably with eosinophils (variable in numbers), and tubular casts (sometimes bright red on trichrome stain). Some of the tubular casts exhibited a yellow tinge or golden brown hue on the H&E stain or a peculiar granular, globular appearance with rounded edges. These myoglobin-containing casts had a classical ultrastructural appearance. In 3 cases, the diagnosis was first suggested by electron microscopy (EM) as the light microscopic features were non-specific. Glomerular and vascular compartments were either entirely normal or reflected findings related to other concomitant pathology.

Conclusions: This study highlights the pathologic findings in patients with AMGURF and emphasizes the value of EM and immunohistochemistry in making the diagnosis and demonstrating the acute proximal tubular injury that is part of the pathologic spectrum in this entity. The lesion is reversible, as long as complicated concomitant renal pathology is not present.

1588 Validation and Utility of Telepathology for Immediate Intraoperative Consultation of Donor Kidney Biopsies

Saba Ali, Alaa Afify, Rajendra Ramsamooj. University of California Davis Medical Center, Sacramento, CA; California Northstate University College of Medicine, Elk Grove, CA.

Background: The immediate intraoperative or bedside evaluation of donor kidneys is a critical step in the procurement of organs for donation. Review by a qualified transplant pathologist poses issues for most medical centers. Telepathology systems enable the electronic transmission of whole slide images for review by a transplant pathologist located at aremote site. We evaluated and validated the use of telepathology for assessment of donor kidneys.

Design: We retrospectively reviewed 25 donor kidney cases with 40 total biopsies. Briefly, intraoperative frozen sections of donor kidneys were prepared and stained with H&E and scanned at 20x using an Aperio CS2 ScanScope®. Scanned whole slide images were interpreted by a transplant pathologist at a remote site. Biopsies were evaluated for: 1) glomerulosclerosis, 2) tubulo-interstitial disease (atrophy, inflammation, and fibrosis), and 3) vascular disease (intimal hyperplasia and arteriolarhyalinosis). The same 40 biopsies were then evaluated by the same pathologist but using conventional light microscopy. The results from the telepathology and light microscopic interpretations were analyzed and compared. Statistical analysis was performed using a McNemar's chi-squared test.

Results: Fifteen percent (6/40 cases) showed a discrepancy in the number of total glomeruli identified by telepathologyversuslight microscope interpretation. There was no statistically significant difference in the percentage of glomerulosclerosis ($P = 0.07$), tubulo-interstitial disease ($P = 0.08$) or vascular disease ($P = 0.13$).

Conclusions: No statistically significant difference was identifiedwhen comparing the degree of glomerulosclerosis and tubulointerstitial and vascular disease using telepathology versus conventional light microscopy. The only difference was the total number of glomeruli identified. This study provides evidence that telepathology is as accurate as light microscopy in evaluating donor kidneys. And, provides relatively easy access to qualified transplant pathologists.

1589 Utility and Patterns of C5b-9 and C4d Immunohistochemical (IHC) Staining in Thrombotic Microangiopathies (TMA)

Mustafa Al-Kawaaz, Steven Salvatore, Surya Seshan. Weill Cornell Medical College, NY, NY.

Background: TMA is microvascular injury and thrombosis, often accompanied by thrombocytopenia and hemolytic anemia. Secondary TMA occurs in association with autoimmune diseases with or without immune complex deposits (ICGN), medications including chemotherapy, transplantation and other less common causes. The variability of etiologies/triggers for atypical and secondary forms of TMA and the stage of renal TMA present a diagnostic and therapeutic challenge as to the underlying pathogenetic mechanism such as complement activation. This study aims to investigate the role of C5b-9 and C4d IHC in renal biopsies with TMA.

Design: 44 patients with TMA on renal biopsy using LM, IF and EM findings. This group was divided into atypical(23) (without a secondary cause), autoimmune (ICGN) (8) and no immune complexes(6), chemotherapy related(7) categories. A control no-TMA group(8) was divided into ICGN(3) and non-ICGN(5) (2 nonrejection transplant bx) categories.

Results: 44 patients (M: 18, F: 26), 2-82 years, presented with elevated creatinine (0.87-11.0mg) and moderate to malignant hypertension. All cases of TMA showed varying degrees of positive staining for C5b-9 (1-3+) within the glomeruli (G), arterioles (Ar), small arteries (SA) and peritubular capillaries (PTC) when compared to no-TMA controls cases ($p=0.003$-0.013). Although C4d was stronger in G in TMA ($p= 0.03$), no significant difference was identified in SA, Ar and PTC, when compared to no-TMA controls ($p=0.66$-0.18). However, all ICGN cases localized strong G staining for C5b-9 and C4d (C5b-9>C4d). While similar intensity (C5b-9>C4d) of G was seen in all other TMA groups without ICGN, mostly negative or focally positive C4d (mainly in active TMA lesions) was noted in the Ar and SA in TMA groups other than the atypical TMA, compared to strong (3+) C5b-9 in all TMA groups (67% vs 95%). In contrast, the PTC displayed diffuse C4d + in 65% of all cases of TMA, whereas focal C5b-9 was noted in only 10% ($p=0.000015$), in both active and chronic TMA. Strong G staining for C5b-9 persisted in all chronic TMA cases as opposed to weaker or no staining for C4d ($p=001$).

Conclusions: Systemic or local complement activation has been implicated in the pathogenesis of TMA and emerging therapies directed against the complement system have produced favorable clinical response. Though the distribution and staining pattern for C4d and C5b-9 are somewhat different, they suggest tissue classical pathway of complement activation in most cases of TMA and ICGN. A combination of C4d and C5b-9 IHC may aid in identification of cases with complement activation.

1590 Apolipoprotein A-IV Amyloidosis Has a Renal Medullary Interstitial Pattern of Deposition – Report of 10 Consecutive Cases

Md Shahrier Amin, Surendra Dasari, Paul J Kurtin, Julie Vrana, Jason D Theis, Sanjeev Sethi. Mayo Clinic, Rochester, MN.

Background: Apolipoprotein A-IV is a rare cause of amyloidosis. There has only been one case report of apolipoprotein A-IV amyloidosis (AAA). The aim of this study was to further characterize the clinicopathological correlates of AAA in the kidney in a bigger cohort of patients.

Design: The Mayo Clinic archives were searched for cases of AAA confirmed by laser microdissection and mass spectrometry. The demographic, clinical and morphological correlates were studied in cases with renal involvement.

Results: Between 2006-2014, apolipoprotein A-IV was detected as the principal amyloid in 30 patients. The organs in which AAA was detected include: kidney – 10 (33%), small intestine – 9 (30%), heart – 8 (26%), lung – 1, skin - 1, both heart and kidney – 1, both heart and mesentery – 1. Among the 10 patients with renal biopsies, 8 were men and 2 women (M:F~4:1). Mean age at diagnosis was 64.5 years. Past medical history was significant for hypertension in 5 and diabetes in 4 patients. 2 patients complained of low back pain. Gradual decline in renal function, with rising serum creatinine (mean at time of biopsy 2.6 mg/dL) was the most common cause for biopsy; proteinuria was absent or minimal (<500 mg/day). Hematological and serological evaluation was negative. The renal biopsy showed moderate to marked quantities of amorphous, homogeneous, glassy eosinophilic deposits restricted to the renal medulla. The deposits were positive on Congo red stain and showed apple green birefringence under polarized light. Immunofluorescence studies were negative in all cases. Electron microscopy showed non-branching fibrils measuring 7-10 nm in thickness. There was no significant cellular reaction to these deposits. Other biopsy findings included mild to moderate arteriosclerosis in 5 patients, moderate interstitial inflammation limited to the cortex in 3 patients and post-infectious glomerulonephritis in 1 patient.

Conclusions: This is the first case-series describing the clinical and morphologic characteristics of renal involvement by AAA. AAA presents with gradual decline in renal function and is characterized by large deposits of amyloid restricted to the renal medulla. The diagnosis may be missed if the sample does not contain medulla. A high degree of suspicion is needed to make the diagnosis of AAA that requires confirmation by laser microdissection and mass spectrometry. Further follow-up and studies are required to elucidate the outcome and appropriate management of renal-limited AAA.

1591 Clinical Significance of Glomerular IgG Deposits in IgA Nephropathy

Nicole Andeen, Anthony S Alvarado, Sergey Brodsky, Alice Hinton, Tibor Nadasdy, Charles Alpers, Christopher Blosser, Behzad Najafian, Brad Rovin. University of Washington, Seattle, WA; Ohio State University, Columbus, OH.

Background: IgA nephropathy (IgAN) involves autoantibodies (IgG or IgA) formed against an autoantigen (galactose-deficient IgA1). Prior research has suggested that the prognosis of IgAN may be adversely affected by co-deposition of IgG in the glomeruli. We sought to better understand the significance of glomerular IgG codeposits in IgAN.

Design: Consecutive IgAN biopsies (n=80) from Ohio State University and University of Washington (2001-2013) were retrospectively classified into IgA and IgA+IgG (IgG > trace). The presence or absence of IgG codeposition was correlated to the combined primary outcome of renal replacement therapy, death, or doubling of serum creatinine (SCr); change in estimated GFR (eGFR) was also assessed. Covariates were age, sex, race, SCr and proteinuria at biopsy, length of follow-up, treatment, Oxford score, and presence of crescents. Renal biopsy findings from cases with available clinical followup and those without (n=95; total n=175) were also analyzed.

Results: The clinical cohort (n=80) was 64% male, 69% Caucasian and 14% Asian. IgA+IgG deposits were seen in 25 of the patients. There was no difference between IgA vs. IgA+IgG with respect to initial or follow-up proteinuria, nor any of the covariates. The primary outcome was reached in 24 patients, 16 with IgA and 8 with IgA+IgG ($p=0.82$). Using multivariate modeling, the change in eGFR over time was

not different between IgA and IgA+IgG. Analysis of renal biopsy findings (n=175) revealed no differences in Oxford score, presence of crescents, nor presence of other immunoreactants in the IgA vs. IgA+IgG groups, nor by comparing groups with C3 deposition vs. those without. Biopsies with crescents/segmental glomerular necrosis (n=65) were associated with endocapillary hypercellularity ($p<0.001$), and deposit location in the peripheral capillary walls in addition to mesangium ($p=0.002$).
Conclusions: In this predominantly Caucasian population with IgAN, glomerular IgG codeposition did not affect clinical outcome.

1592 PLA2R Negative De Novo Membranous Nephropathy Associated with Antibody-Mediated Rejection; a Report of 11 Cases with Common Light Microscopic and Ultrastructural Features

Siripron Angchuan, Mongkon Charoenpitakchai, Jittirat Arksarapuk, Agnes B Fogo, Paisit Paueksakon. Vanderbilt University Medical Center, Nashville, TN; The Queen's Medical Center, Honolulu, HI.
Background: Membranous nephropathy (MN) in the renal allograft can occur either as a recurrence of primary disease or de novo. Antibodies to PLA2R have been associated with some cases of recurrent MN, but the data thus far are limited. In contrast, the pathophysiology of de novo MN is not clearly understood but may be associated with antibody-mediated rejection (ABMR) in the allograft.
Design: Biopsies of 17 patients with MN in the transplant biopsy who had a tissue diagnosis/clinical history reviewed at VUMC documenting the primary native renal disease were studied. Morphologic evaluation and PLA2R staining was performed.
Results: 11 pts (64%) had de novo MN and 6 pts (36%) had recurrent MN. 2/6 (33%) pts with recurrent MN showed microcirculation inflammation (MCI), in contrast to MCI in all pts (100%) with de novo MN. In recurrent MN, PLA2R was positive in 4/6 (67%) pts, in contrast to de novo MN, where none (0%) showed PLA2R positivity. C4d was positive in 1/6 (17%) pts with recurrent MN and 3/11 (27%) with de novo MN. Donor specific antibodies were positive in 1/2 (50%) pts with available data in recurrent MN and 2/3 (67%) in de novo MN. In both recurrent and de novo MN, all pts (100%) by definition showed subepithelial (SEP) deposits by EM, and IgG and C3 staining by IF. There was no evidence of transplant glomerulopathy (TGP), multilayering of peritubular capillary basement membranes (PTC), subendothelial (SEN) or mesangial (M) deposits in recurrent MN (0%). However, in de novo MN, 10/11 (91%) showed multilayering of PTC and of these; 6 (55%) showed TGP, and of these; 5 (45%) showed M and/or SEN deposits by EM.
Conclusions: PLA2R staining was found in most recurrent MN patients but in none of de novo MN, supporting a distinct pathogenesis of de novo MN in the transplant. Most patients with de novo MN had MCI, PTC basement membrane multilayering, TGP, M and/or SEN deposits. These common LM and EM features support antibody-mediated rejection as an underlying etiology of de novo MN. Furthermore, M and SEN deposits are new findings which have not previously been described in MN associated with ABMR, raising the possibility that circulating immune complexes may deposit on the luminal side of the GBM and in the mesangium, disassociate, and reform in a subepithelial position. We further conclude that these common LM and EM findings together with negative PLA2R are surrogate markers for MN associated with ABMR.

1593 Prevalence of Glomerular Disease Recurrence in Renal Allografts: A Single Center Study

Brad Barrows, Vighnesh Walavalkar, Zoltan Laszik, Kuang-Yu Jen. University of California San Francisco, San Francisco, CA.
Background: Glomerular disease is responsible for a significant proportion of end-stage renal disease (ESRD) in the United States. About 10-15% of ESRD is caused by glomerulonephritis (GN), and diabetic nephropathy (DN) is the most prevalent renal disease with glomerular manifestations, accounting for over half of ESRD cases. Given that glomerular disease is the etiology for ESRD in a large proportion of renal transplant patients, glomerular disease recurrence in renal allografts is not uncommon. Determining the specific glomerular diseases that recur most frequently can help nephrologists identify patients that may require close follow-up and treatment after transplantation for disease recurrence. In this study, we retrospectively analyzed renal allograft biopsies performed at our institution from 1994 through 2015 to determine the prevalence and trends over time of various types of recurrent glomerular diseases in renal allografts.
Design: Renal allograft biopsy reports were reviewed for the diagnosis of recurrent glomerular disease between 1994 and 2015 at our institution. The cases of recurrence were then stratified by diagnosis and year of biopsy, the latter of which was divided into two separate decades(1994-2004 and 2005-2015).
Results: In total, 448 cases of recurrence were identified out of 6850 allograft biopsies (6.5%). Between 1994 and 2004, 159 cases of recurrent disease were identified out of 862 allograft biopsies (18.5%), while 289 of 5988 allograft biopsies were found to have recurrent disease from 2005 to 2015 (4.8%). The most common recurrent diseases included focal segmental glomerulosclerosis (FSGS; 36%), IgA nephropathy (25%), DN (13%), membranoproliferative GN (MPGN; 7%), and membranous GN (6%). Comparing 1994-2004 to 2005-2015, the proportion of recurrent cases showing FSGS decreased (42% vs. 34%) while those with DN and MPGN increased (9% vs. 14% and 3% vs. 7%, respectively), although these trends did not reach statistical significance.
Conclusions: The overall frequency of renal allograft biopsies that showed recurrence has decreased over time at our institution, likely due to a drastic increase in protocol biopsies (i.e. routine biopsies performed not triggered by clinical cause). However, a sizeable proportion of renal allograft biopsies showed glomerular disease recurrence with FSGS being the most common. Comparing biopsies performed in 1994-2004 and 2005-2015, the proportion of recurrent cases showing specific categories of glomerular disease demonstrated no statistically significant differences, although some trends were noted.

1594 Membranous Glomerulonephritis with Monotypic IgG Deposits: A Clinico-Pathological Analysis of 28 Cases

Alejandro Best Rocha, Christopher Larsen. Nephropath, Little Rock, AR.
Background: Membranous glomerulonephritis (MGN) is the most common cause of nephrotic syndrome in Caucasian adults. While the majority of cases are caused by polytypic deposits, cases with light chain restricted IgG deposits may be rarely seen. Monotypic IgG deposition in the setting of proliferative glomerulonephritis is well described in large case series and has been shown to not have an underlying lymphoproliferative disorder (LPD) in most cases. However, the significance in light chain restricted MGN is yet to be determined. We present a series of 28 cases of glomerulonephritis with a predominantly membranous pattern and monotypic IgG deposits.
Design: A retrospective analysis with clinico-pathological correlation was performed of all cases of MGN with monotypic IgG deposits diagnosed at our institution between 01/2010 and 09/2015.
Results: A total of 28 biopsies from 26 patients were reviewed. The mean age at diagnosis was 63.1yr (37–87yr) and the male to female ratio was 1. All patients presented with proteinuria (69.2% in nephrotic range) and the mean serum creatinine was 1.44 mg/dl (0.4–5.0 mg/dl). Histologically, all cases showed predominantly a membranous pattern, with 4 (14.3%) showing focal endocapillary proliferation with or without crescents. Kappa light chain restriction was seen in 24/28 of the biopsies (85.7%), while the remaining 4 showed lambda restriction. IgG subclasses performed in 17/28 cases showed monoclonality in 13 and biclonality in 4 (see table). PLA2R was positive in 6/25 cases. IgG subclasses were available in 3 of the PLA2R positive cases, all of which were biclonal. Follow-up data was available in 17/26 patients. Five patients had or developed a clinical diagnosis of a LPD (predominantly CLL) and one of an autoimmune disorder. Only one patient with LPD had a detectable paraprotein, consistent with the phenotype of the glomerular deposits. 3/5 patients with LPDs had focal endocapillary proliferation, one of them with cellular crescents. None of the patients were positive for hepatitis C, and only one was positive for hepatitis B.

Monoclonal (n=13)		Biclonal (n=4)	
IgG1κ	4	IgG1κ + IgG2κ	1
IgG2κ	2	IgG1κ + IgG3κ	1
IgG3κ	3	IgG1κ + IgG4κ	2
IgG4κ	1		
IgG1λ	3		

Conclusions: The majority of cases of MGN with monotypic IgG deposits lack a recognizable secondary etiology. A subset of these patients (19.2%), however, have an associated LPD, predominantly CLL. Therefore, when monotypic deposits are identified on renal biopsy, the presence of a concomitant LPD should be ruled out, even in the absence of a recognizable paraprotein.

1595 Abstract Withdrawn

1596 Apolipoprotein L1 (ApoL1) High-Risk Variants Correlate with Parietal Epithelial Cell Activation among African Americans with Arterionephrosclerosis

Justin H Chen, Huma Fatima, Haichun Yang, Agnes B Fogo. Vanderbilt University Medical Center, Nashville, TN; University of Alabama at Birmingham, Birmingham, AL.
Background: ApoL1, a small lipoprotein, can filter through glomerular basement membranes, and reach and potentially be reabsorbed by podocytes, parietal epithelial cells (PEC), and tubular epithelial cells. SRB1 is a major transporter for lipoprotein. Recently, risk allele variants of the ApoL1 gene, commonly present in African Americans (AA) (G1, G2) but very rare in Caucasians (C) who express G0 variants, were implicated in podocyte injury-related kidney disease, such as FSGS. Activated PECs express CD44, and may migrate to the glomerular tuft and replace podocytes, or contribute to sclerosis. Previous data suggest ApoL1 risk variants contribute to glomerulosclerosis in arterionephrosclerosis in AA. However, whether ApoL1 risk variants affect PEC function and SRB1 is unknown.
Design: Kidney biopsies with a diagnosis of arterionephrosclerosis were identified (n=56), genotyped for the presence of the high risk ApoL1 gene variant, and assessed for pathological lesions, CD44 and SRB1 immunostaining.
Results: Our population included 19 C (11 male/8 female) and 37 AA patients (23 male/14 female), on average 56.3 ± 2.2 yrs. Amongst AA patients, 20 had 0 risk alleles, 9 had 1 risk allele and 8 had 2 risk alleles. None of the 19 C patients had risk alleles. C and AA patients with 0 risk alleles had similar morphologic features. AA patients with 1 or 2 risk alleles showed more global glomerulosclerosis (GS) (50.5 ± 7.2 vs. 37.2 ± 5.9%), but no difference in segmental GS, mesangial expansion and podocyte effacement compared to AA without risk alleles. In AA without risk alleles, 6.7% of glomeruli showed CD44 positivity in visceral epithelial cells and 6.2% of glomeruli showed positivity in PEC. In AA with risk alleles, this positivity increased to 9.9% and 11.7%, respectively. PEC showed rare expression of SRB1 in normal kidney, but 32.7% of glomeruli expressed strong SRB1 in PEC in AA without risk alleles, vs. 59.5% in AA with risk alleles. These SRB1 positive PECs were located not only in segmental GS, but also in normal glomeruli.
Conclusions: Patients with arterionephrosclerosis and high-risk variants of ApoL1 have more PEC activation, which may correlate to increased glomerulosclerosis. We hypothesize that higher expression of SRB1 induces more ApoL1 absorption and PEC activation in these patients.

1597 Dendritic Cells in Renal Biopsies of Patients with Light-Chain Mediated Tubular Interstitial Nephritis

Mingyu Cheng, Guillermo A Herrera. Louisiana State University Health Sciences Center, Shreveport, LA.

Background: Dendritic cells (DCs) play a critical role in the regulation of the adaptive immune response and can be separated into two major subsets: myeloid and plasmacytoid DCs. Their involvement in light-chain mediated tubular interstitial nephritis (LC-TIN) is unknown. In this study, the participation and localization of DC subsets were investigated in LC-TIN.

Design: A total of 25 renal biopsies from patients with LC-TIN (n=8), lupus nephritis (n=9, positive controls), or minimal change diseases (MCD, n=8, negative controls) were studied. All biopsies were investigated with direct immunofluorescence (DIF) for myeloid (CD1c) and plasmacytoid (CD303) DC subsets. The amount of DCs in the biopsies was determined by area measurement using the digital image analysis system ImageJ. Positively stained area was expressed as a fraction of the area of the high power field examined. Maturation state of DCs was investigated with double immunofluorescent staining of CD80 and a DC marker (CD1c or CD303). The ultrastructural features of DCs in renal biopsies were evaluated by transmission electron microscopy (TEM).

Results: DCs were identified morphologically within the tubulointerstitium in the renal biopsies by TEM interacting with surrounding tubules and inflammatory cells. CD1c positive cells and CD303 positive cells were identified in the biopsies of all three groups by DIF staining. LC-TIN had significantly increased CD1c positive cells (6.27%±0.91%) and CD303 positive cells (4.12% ±0.54%) as compared to MCD (CD1c: 1.01%±0.69%, p<0.01; CD303: 0.65%±0.34%, p<0.01) and lupus nephritis (CD1c: 2.23%±0.43%, p<0.01; CD303: 1.93%±0.38%, p<0.01). CD1c and CD303 positive cells in biopsies with LC-TIN were exclusively restricted to the tubulointerstitium. Co-expression of CD80 was identified on some CD1c positive cells in LC-TIN, whereas only few CD303 positive cells were found to co-express CD80.

Conclusions: Both myeloid and plasmacytoid DCs are significantly increased in the tubulointerstitium in LC-TIN as compared to those in MCD and lupus nephritis, suggesting these two subsets of DCs may be important in the inflammatory process of LC-TIN. Some mature CD1c positive DCs were identified in LC-TIN by their co-expression of CD80, whereas only few CD303 positive DCs were found to co-express CD80, suggesting DC subsets may be differentially involved in the pathogenesis of LC-TIN.

1598 Characterizing the Inflammatory Infiltrate in Human Kidney Biopsies with TIN

Hae Yoon G Choung, Liying Fu, Ekaterina Castano, Natalie Patel, Gilbert Moeckel. Yale University School of Medicine, New Haven, CT; Yale School of Medicine, New Haven, CT.

Background: The outcome of tubulointerstitial nephritis (TIN) is determined by inflammatory infiltrate, which drives progression of renal failure towards end stage renal disease (ESRD). Most diabetic nephropathy (DN) biopsies show a TIN component. Studies investigating TIN have focused on pro-inflammatory T-cells and only a few have analyzed other inflammatory components. The goal of this study is to characterize the components of the inflammatory infiltrate in kidney biopsies of patients with TIN +/- DN, and to correlate these results with parameters of renal function and progression of fibrosis.

Design: Copath and Epic databases were searched at our institution to identify human kidney biopsies with TIN, with or without DN. 75 cases with active TIN were identified of which 26 had also DN. H&E and immunohistochemical stains for leukocyte subtypes were reviewed and analyzed by two pathologists. Cases were separated based on extent of interstitial fibrosis (IF): group 1 ≤ 50% IF and group 2 > 50% IF.

Results: Of the TIN +DN cases, group 1 (n=7) had more regulatory T cells than group 2 (n=19); (0.6±1.2/HPF vs 0.1±0.3/HPF; p< 0.05; t-test; n=17). Within the TIN -DN cases (n=49), group 1 (n=23) had less global glomerular sclerosis (24.3±24.5% vs. 49.4±35.7%) and lower creatinine levels (2.53±0.67 vs. 4.04±2.47) compared to group 2 (n=26). Comparing the cases in group 2 of TIN –DN vs TIN +DN, we found less CD8+ T-cells (23.3±14.8/HPF vs. 42.9±25.5/HPF, n=20) and significantly more M2a macrophages (22.4±15.6/HPF vs 5.03±6.4/HPF; p<0.05, t-test, n=22) in the TIN –DN group.

Conclusions: M2a macrophages and T-regs are anti-inflammatory leukocytes needed for abating further renal damage in TIN. In our cases of TIN +DN with less than 50% IF, we found increased T-reg concentrations. This could reflect recruitment of anti-inflammatory cells at times of intense inflammation to prevent IF. In addition, we found that TIN –DN biopsies with more than 50% IF, had significantly more M2a macrophages and less CD8+ T-cells, compared to TIN +DN with similar degree of IF. This indicates a role of M2 macrophages in decreasing CD8+ T-cells, which are cytotoxic effectors of tissue injury, thus preventing tissue damage. DN may have an augmenting effect on CD8+ T-cell recruitment, thus enhancing chronic tissue damage. The findings in this study suggest that there are subsets of inflammatory cells in TIN that have an important protective function against chronic tissue injury.

1599 Maximizing Information from the Renal Biopsy: Computer-Generated Three-Dimensional Constructs

Beverly E Faulkner-Jones, Devin Rosen, Seymour Rosen, Kyle Harrington, Charles Law. BIDMC, Boston, MA; Kitware Inc, Clifton Park, NY.

Background: Tubular elements in the renal biopsy undergo a complex synchronous process of hypertrophy, atrophy and cyst formation. The shape shifts generated are diverse and difficult to categorize and quantitate using conventional microscopy. We present three-dimensional constructs developed from such tubules. A biopsy from a patient with lithium nephrotoxicity was chosen because of the full representation of these changes.

Design: The renal biopsy was serially sectioned and stained (H&E, PAS, Jones, trichrome, CD31, AE1/AE3-CAM5.2), digitized (Philips UFS) and the sequential whole slide images (WSIs) viewed on https://slide-atlas.org. Serial WSIs were aligned, and the regions of interest segmented, extracted and volume-rendered for further analysis.

Results: Typical changes of lithium toxicity were seen: cysts, tubular atrophy and hypertrophy. All these changes were all more easily appreciated by rapid sequential viewing of aligned WSIs. 3D volumes of selected larger cysts, and groups of hypertrophic or atrophic tubules were generated and compared with respect to their relative size and shapes (Figure 1). Estimated volumes of the larger cysts were 10-fold greater than those of the hypertrophic tubules, which in turn were 10-fold greater than those of the atrophic tubules.

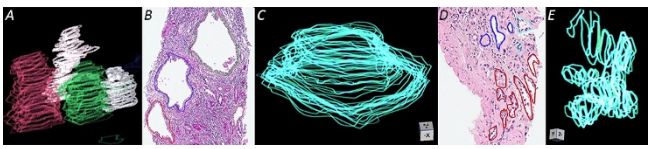

Figure 1. Segmented, volume-rendered large cysts (A-C) and a group of atrophic tubules (D,E). 3D volumes (A) were generated from large cysts (B). The top cyst shown in (B) is represented in (C) and has an estimated total volume of 0.126 mm3. A group of atrophic tubules (D) has unexpected complexity and continuity in three dimensions (E).

Conclusions: These studies show a wide range of shape shifts in tubular elements. Representation of actual cyst size within the renal parenchyma can be calculated. These studies are the first of this type and serve to advance the better understanding of chronic renal disease.

1600 Capsulitis: A Novel Histologic Correlate in T-Cell Mediated Rejection

Alexander J Gallan, Kammi J Henriksen, Anthony Chang. The University of Chicago, Chicago, IL.

Background: Acute T-cell mediated rejection (TCMR) is an important cause of renal allograft loss. The Banff schema classifies TCMR based on the degree of lymphocytic infiltration of the tubules (types IA and IB) and arteries (types II and III), which correlates with allograft function and survival. However, lymphocytes can also occasionally be identified on the intraglomerular aspect of Bowman capsules (or "capsulitis"), which has not been previously described. This study was undertaken to define the novel histologic feature of "capsulitis" and delineate its clinicopathologic relevance in TCMR of kidney allografts.

Design: We identified renal biopsies with TCMR at our institution from 2010-2015. Exclusion criteria included repeat biopsies from the same patient, presence of <7 glomeruli, and concomitant polyoma virus nephropathy. The cases were assessed for capsulitis, defined as the presence of one or more lymphocytes between Bowman capsules and parietal epithelial cells in a single non-globally sclerosed glomerulus. The 2013 Banff classification was applied. Clinicopathologic variables were compared using Chi-square test.

Results: A total of 72 cases of TCMR were identified. There was no significant difference in age, sex, graft age, or serum creatinine level at time of biopsy between the cases with and without capsulitis. Table 1 shows the relationship between Banff grading and capsulitis.

Banff Type	n	Capsulitis +
Borderline only	1	0
IA only	25	11 (44%)*
IB only	17	15 (88%)*
Borderline + II or III	3	2 (67%)
IA + II or III	4	2 (50%)
IB + II or III	10	9 (90%)
II or III only	12	9 (75%)
Total	**72**	**48 (67%)**
		*p<0.01

Capsulitis could occur mechanistically as an ascending progression of tubulitis through the urinary pole and into Bowman capsule. However, we also identified capsulitis in isolated Banff II and III cases, and noticed type IA cases with capsulitis and ischemic fraying of Bowman capsules. This raises the possibility of a second potential mechanism of direct penetration of lymphocytes despite the increased thickness of Bowman capsule compared to the tubular basement membrane.

Conclusions: This study describes a novel histologic feature of "capsulitis" in TCMR of renal allografts. We found that capsulitis was more commonly associated with Type IB than IA TCMR, suggesting that capsulitis may be a marker for more severe TCMR. Additional studies are necessary to further delineate the pathologic and clinical relevance of "capsulitis" in acute TCMR of renal allografts.

1601 Routine Clinical Use of Exome NGS for Diagnosis in Patients with Renal Disease

Joseph Gaut, Sanjay Jain, John D Pfeifer, Catherine E Cottrell. Washington University, St. Louis, MO.

Background: The state of the art in renal pathology relies on light, immunofluorescence, and electron microscopy (LIEM). However, in selected patients, this combination of techniques is insufficient to make a firm diagnosis. Since a subset of renal diseases (e.g. nephrotic syndrome, atypical hemolytic uremic syndrome (aHUS), cystic diseases) are increasingly recognized to harbor genetic mutations responsible for the disease or that serve as disease risk factors, next generation sequencing (NGS) as part of routine clinical practice has potential to increase diagnostic accuracy.

Design: Cases for which the results of traditional LIEM analysis were not definitive were referred for germline NGS sequencing as part of routine patient care (via exome-based DNA sequencing using a hybrid capture approach, and an Illumina HiSeq2500 with paired 2x101bp reads). Sequence analysis included 25 genes associated with the following diagnostic groups: aHUS, nephrotic syndrome, Alport syndrome, and metabolic disorders. The NGS was performed in a CAP accredited/CLIA licensed clinical laboratory, and the results were reviewed by a board certified molecular pathologist/geneticist prior to release to the patient's medical record.

Results: To date, NGS has been performed as part of routine clinical care in 23 patients referred for aHUS evaluation and 3 referred for nephrotic syndrome. Of the aHUS patients, identified sequence changes include 7 single nucleotide variants (1 novel pathologic variant in CFH and 6 variants of unknown significance (VUS) in CFH, CFI, CFB, C3, and THBDx2) and 8 indels (heterozygous deletions in CFHR3/CFHR1 in 4 patients and homozygous deletions in CFHR3/CFHR1 in 4 patients). Of the nephrotic syndrome patients, 2 single nucleotide variants were identified (VUS in LAMB2 and ACTN4), but all cases were negative for APOL1 risk alleles. In order to support identification of associations between identified sequence variants and pathogenesis in cases for which traditional LIEM is not definitive, a registry of all referred cases has been established.

Conclusions: VUS represent the largest category of identified genetic variants among patients with aHUS and nephrotic syndrome. Thus, elucidation of disease associations between sequence variants in cases for which traditional LIEM is not definitive will require correlation of NGS results with other genetic, phenotypic, and clinical parameters. Partnerships among groups that perform NGS sequencing as part of routine clinical care will help to rapidly expand this database.

1602 Spectrum of Glomerular Lesions in Native Renal Biopsies with TRIs

Rajib Gupta, Serena Bagnasco, Naima Carter-Monroe, Lois Arend. Johns Hopkins University, Baltimore, MD.

Background: Tubuloreticular inclusions (TRIs) are small clusters of anastomosing tubule-like structures most commonly found in the cytoplasm of endothelial cells. They suggest elevated interferon levels associated with viral infection, autoimmune disorder, or rarely drugs (most commonly interferon therapy). We present a 10-year study of the prevalence of TRIs in glomerular diseases from all native biopsies received.

Design: Native kidney biopsies from 2005 to 2015 were reviewed for presence of TRIs. The biopsies were divided into lupus (sub-divided into established lupus, past history of lupus, or suspicious for lupus), viral infections (sub-classified into HIV, HCV, HBV, or a combination) and an "other" category.

Results: 250 cases were found with TRIs. 126 cases fell into one of the lupus sub-categories (50%), 68 cases had one or more of the 3 viral etiologies (27%), and 56 belonged to the other category (22%). Among the 126 lupus cases, 97 were established lupus cases, 22 were suspicious for lupus, and the remaining 7 were patients with a past history of lupus. Biopsies with Class III, IV, and V had the highest prevalence of TRIs. In the infectious category of biopsies with TRIs, 26 cases had HIV, 22 cases had hepatitis C, 16 had both HIV and HCV, one case had both HCV and HBV, and 1 case was positive for all 3 viruses. In the other category, multiple myeloma was present in 5 cases; minimal change disease was present in 7 cases, 7 cases had diabetic nephropathy, 10 cases had focal segmental glomerulosclerosis, 3 cases had an autoimmune connective tissue disorder other than lupus, most commonly rheumatoid arthritis; 5 cases had membranous nephropathy, 3 were IgA-dominant post-infectious glomerulonephritis, 3 cases were ANCA-associated glomerulonephritis, 1 case had a diagnosis of Alport syndrome and 1 other was suspicious of Alport, 1 case of hypertensive renal vascular disease, 1 case each of thrombotic microangiopathy and Henoch-Schonlein purpura, and 4 cases were idiopathic.

Conclusions: TRIs are an electron microscopic feature found in a variety of glomerular diseases. While they appear when interferons are elevated for various reasons – infection, immune dysfunction, exogenous interferon therapy, or drug-induced increase in interferon level, they are found in numerous settings not typically associated with high levels of interferon, which may indicate an as yet unknown pathogenesis.

1603 Dendritic Cells in Renal Allografts

Meghan Kapp, Sharon Phillips, Deborah O Crowe, Jorge Garces, Agnes B Fogo, Giovanna A Giannico. Vanderbilt University Medical Center, Nashville, TN; Vanderbilt University, Nashville, TN; DCI Transplant Immunology Laboratory, Nashville, TN; Ochsner Health System, New Orleans, LA.

Background: Dendritic cells (DCs) are antigen presenting cells that initiate primary T-cell response and activate memory T-cells. DCs are classified into two major subsets: myeloid DC (mDC)(BDCA1+DC-SIGN+ and BDCA1+DC-SIGN-) and plasmacytoid DC (pDC)(BDCA2+DC-SIGN-). DC-SIGN+ mDCs secrete IL-12, signaling naïve CD4+ T cells to T-helper (Th)-1 phenotype. BDCA2+ pDCs produce proinflammatory cytokines. In this study, we evaluated DC subtypes, markers of endothelial activation, and Th subsets by immunohistochemistry (IHC) in renal transplant biopsies with the hypothesis that DC populations are differentially upregulated in antibody-mediated rejection vs. controls. Further, we studied the association of intragraft DC subtypes with endothelial activation and FOXP3/STAT3 ratio.

Design: IHC for markers of DC subtypes (BDCA1, DC-SIGN, BDCA2), endothelial activation (P- and E-selectins) and T-cell subtypes (FOXP3 and STAT3) was performed on 75 renal transplant biopsies, two categories with evidence of ABMR, C4d+DSA+ (n=35) and C4d-DSA+ (n=23), and ABMR negative C4d-DSA- (n=15, CTR), all with variable microvascular injury (MI), and 2 normal kidneys (NL). Positive cells were counted and normalized to cortex area (ScanScope CS, Aperio v11.2.0.780). Statistical analysis was performed using Kruskal-Wallis and Wilcoxon rank-sum tests.

Results: BDCA2+pDCs were significantly higher in C4d+DSA+, C4d-DSA+, and CTR compared to NL. DC-SIGN+ mDCs were significantly increased in CTR compared to all other groups and NL. BDCA2+ and DC-SIGN+ DCs were significantly associated with the expression of markers of endothelial activation (P- and E-selectin). DC markers did not associate with FOXP3/STAT3 ratio. DC-SIGN expression was higher in cases with Banff C4d score 0-1 vs. 2-3 and negative vs. positive DSA status ($p=0.032$ and < 0.001, respectively).

Conclusions: BDCA2+ pDCs were elevated in all transplant patients with MI regardless of DSA status or level of C4d positivity compared to NL, while DC-SIGN+mDCs were higher in CTR with negative C4d and DSA. These findings suggest that BDCA-2 could have a pro-inflammatory effect in triggering humoral rejection response, while DC-SIGN+mDCs could exert a protective, and indirectly, tolerogenic effect. This effect may be independent of the FOXP3/STAT3 ratio and may be associated with intragraft endothelial activation mechanisms.

1604 Clinicopathologic Correlation of Acute Kidney Injury in Human Patients

Satoru Kudose, Masato Hoshi, Sanjay Jain, Joseph Gaut. Washington University in St. Louis, St. Louis, MO.

Background: Clinical acute kidney injury (AKI) diagnosis relies on the insensitive biomarkers serum creatinine (SCr) and urine output. Several groups have used these biomarkers to standardize AKI diagnosis including the Acute Kidney Injury Network (AKIN), Kidney Disease Improving Global Outcomes (KDIGO) and European Renal Best Practice (ERBP). However, little is known about the relationship between clinical AKI definitions and pathologic kidney injury. It is the aim of this study to correlate clinical AKI with pathologic kidney injury in human patients.

Design: Our pathology archives were searched for native kidney biopsies obtained with and without clinical AKI. 55 biopsies were identified, 41 with and 14 without clinical AKI. The biopsies were examined, blinded to clinical data, for pathologic findings of tubular injury and their extent. Immunohistochemical staining for Kidney Injury Molecule-1 (KIM-1) was performed on cases with AKI (grade 3) and without AKI and scored as number positive tubules per 500 tubular cross sections. Correlation between pathologic findings, KIM-1 staining, and clinical AKI defined by the KDIGO and ERBP modified AKIN criteria was performed using Spearman's rank-order correlation. Pathologic tubular injury was assessed using Fisher's exact tests.

Results: Using the KDIGO criteria, clinical AKI was strongly correlated with extent of morphologic tubular injury ($r=0.76$). By ERBP criteria, clinical AKI showed moderate correlation ($r=0.55$). KIM-1 staining strongly correlated with severe clinical AKI by the KDIGO and ERBP criteria ($r=0.75$). The proportion of tubules with KIM-1 staining correlated with extent of morphologic tubular injury ($r=0.66$). The following tubular histologic changes were associated with clinical AKI (KDIGO): brush border loss, cytoplasmic blebbing, epithelial simplification, and mitoses ($p<0.0005$). KIM-1 staining showed strongest correlation with tubular dilatation, tubular epithelial simplification, tubular mitoses, tubular cell sloughing, and tubularization of Bowman's capsule (all $p<0.02$).

Conclusions: Amongst patients who underwent renal biopsy, morphologic tubular injury correlates best with clinical AKI using modified KDIGO criteria. KIM-1 immunohistochemistry correlates with morphologic tubular injury and clinically severe AKI. Discrepancies may be related to sampling error or may reflect the functional nature of SCr as an injury biomarker.

1605 Quantitative Real-Time PCR as a Surrogate Method to Detect BK Virus (BKV) in Renal Transplant Biopsies with Negative SV-40 Staining

Tripti Kumar, Rebecca Sovoda, John Gibson, Sarah Britton, Andrea J Shaw, Bobby Boyanton, Dilip Samarapungavan, Ping L Zhang. Beaumont Health System, Royal Oak, MI.

Background: Scattered studies using quantitative real-time PCR (qPCR) for BKV in renal tissue suggest feasibility of the technique for detecting BKV, however, no clinical utility of qPCR for BKV using renal tissue has been implemented. When SV40 staining is negative in a biopsy while the patient has high serum or urine BKV, it is a dilemma how to give an accurate diagnosis and to treat the patient. This investigation was to determine whether qPCR from paraffin embedded tissue could enhance the detection of BKV in renal grafts biopsies with negative SV40 staining.

Design: Thirteen negative controls (4 tonsils, 2 native kidney biopsies, 7 renal transplant biopsies with 3 acute tubular injury, 3 acute cellular rejection and 1 antibody mediated rejection), 5 positive controls (1 bladder biopsy, 4 renal graft biopsies with known positive SV40 staining) and 5 uncertain cases (high clinical suspicion with high urine/serum BKV and negative SV40 staining) were selected for the study. DNA was extracted from each specimen using five 5-µm curls from the formalin-fixed parafin-embedded tissue block using the QIAamp DNA FFPE Tissue Kit (Qiagen) for BKV qPCR (The qPCR linear range is 500 to 500 x 10^6 copies/mL).

Results: BKV was not detected in the tonsillar and native kidney biopsies. BKV was detected (10 copies/ng DNA) in the negative control renal transplant biopsies. Except one positive case with minimal renal tissue left showing 2.5 copies/ng DNA, the remaining 4 positive cases had high pairs of BKV ranging from 5,263 to 160 million copies/ng DNA. In five uncertain cases, there were low BKV levels, ranging from 160 to 277 copies/ng DNA in 3 cases with rejection diagnosis in the reports (low suspicion), but 0.19 to 0.53 million BKV copies/ng DNA in the remaining two cases (high suspicion).
Conclusions: Our data demonstrate that qPCR BKV testing from paraffin embedded tissue is very sensitive for ruling in/out BKV in renal transplant biopsies. Based on our preliminary data, cut-off values of < 10, 10 to 500 and >500 copies/ng DNA may represent absence, low suspicion and high suspicion for the presence of BKV in biopsies, respectively.

1606 Comparison of Renal Biopsy Pathology in Adults and Children with Systemic Lupus

Li Lei, Craig Zuppan. Loma Linda University Medical Center, Loma Linda, CA.
Background: Evaluation of kidney involvement in patients with systemic lupus erythematosus (SLE) is one of the more common indications for renal biopsy. However, there have been few recent studies comparing the biopsy features of SLE in children to those in adults.
Design: We undertook a single institution retrospective review of all renal biopsies from patients with SLE performed between 2004 and 2014. All biopsies were reported and studied by a single renal pathologist (cz).
Results: A total of 251 biopsies were identified from patients indicated to have SLE. 8 cases were excluded from the study: 7 because the biopsy was inadequate for evaluation of glomerular disease, and one because the patient's lupus had been inactive for many years. The final study group included 117 children (≤ 18 years of age) and 126 adults (> 18 years). Gender was overwhelmingly female in both groups (83% of pediatric, and 88% of adults). Indications for renal biopsy included proteinuria, hematuria, acute or chronic renal insufficiency, follow-up comparison, and mixtures of the above. The stated indication for biopsy in children was less often renal insufficiency (3.4% vs. 15.1%), and more often for follow-up after interval therapy or development of new clinical findings (45% vs. 31%), as compared to adults.
ISN/RPS class distribution for pediatric versus adult biopsies were as follows: Class I-II, 8.5% vs. 6.3% (P=0.51); Class III, 30.8% vs. 13.5% (P<0.01); Class IV, 36.8% vs. 43.7% (P=0.27); Class V, 5.1% vs. 14.3% (P=0.02); and Class VI, 1.7% vs. 4.8% (P=0.33). Other diagnoses not falling within the ISN/RPS classification included one adult patient each with thrombotic microangiopathy and minimal change nephropathy. Chronic changes were less frequent in the pediatric biopsies, as measured by the frequency of >50% tubular atrophy (8.1% vs, 25%, P<0.01). Comparison of NIH activity and chronicity scores showed mean activity scores in the two groups of 4.1±0.3 and 4.4±0.3, and mean chronicity scores of 2.1±0.2 versus 4.2±0.2. Crescents and wire loops were somewhat less common in the pediatric biopsies (22.4% vs. 34.1%, P=0.04 and 28.4% vs. 31.7%, P=0.58, respectively).
Conclusions: The findings on renal biopsy for SLE are fairly similar in children and adults, although children tend to have less advanced chronic changes, less frequent crescents and wire loop lesions, and less commonly develop membranous lupus nephritis.

1607 C3 Glomerulopathy in Older Adults

Isaac Lloyd, Hunter Huston, Stephen Jenkins, Kalani Raphael, Dylan Miller, Monica P Revelo, Mazdak Khalighi. University of Utah, Salt Lake City, UT.
Background: C3 glomerulopathy (C3GP) includes both C3 glomerulonephritis (C3GN) and dense deposit disease (DDD) and is defined by C3-dominant deposits by immunofluorescence. Abnormal function of the alternative pathway (AP) of complement is central to the pathophysiology of C3GP and young patients often harbor genetic alterations of mediators of AP. Recently, a link between C3GP and paraproteinemia has been established, but the frequency of this association in older patients is not well characterized. To explore this, we studied C3GP specifically in adults > 50 years in age.
Design: 13 biopsies from 11 patients meeting diagnostic criteria for C3GP were identified in patients over the age of 50 from 2005-2015. Pathologic and clinical features were reviewed, including the presence of a monoclonal gammopathy and/or lymphoma or plasma cell dyscrasia.
Results: C3GP accounted for 1.8% of biopsies in patients > 50 years during the study period. 73% of patients were male and the median age was 63 (range: 52-90) years. The mean serum creatinine at presentation was 2.75 (range: 1.2-10) mg/dL and mean proteinuria was 3.1 (range: 0.1-10) g/day. Hematuria was universally present. A paraprotein was identified in 8 patients (7 IgG-κ, 1 IgG-λ) and 1 additional patient was diagnosed with classical Hodgkin lymphoma 6 months prior to diagnosis of C3GN. Of the patients with paraproteinemia, 3 had myeloma on bone marrow biopsy, 2 had monoclonal gammopathy of undetermined significance (MGUS), and 1 had a polyclonal plasmacytosis. On kidney biopsy, 9 showed MPGN, 3 showed mesangioproliferative GN, and 1 showed a focal exudative GN. Ultrastructural findings diagnostic of DDD were seen in 1 patient with MPGN and 1 with mesangioproliferative GN. The biopsy showing focal exudative GN represented recurrent disease in an allograft. Mean follow up was 3.1 years (range: 1 month-10 years). 5 patients required chronic renal replacement therapy (RRT), 1 of which passed away soon after the diagnosis of C3GP and Hodgkin disease. 5 patients had stable chronic kidney disease (CKD) at last follow-up. 1 patient, who presented with acute kidney injury, underwent bone marrow transplant for multiple myeloma and had baseline kidney function one year post transplant.
Conclusions: C3GP is an uncommon but important cause of kidney injury in older adults as 45% of patients in our cohort required RRT and all but 1 had CKD at follow-up. Given that over 80% of patients demonstrated a monoclonal gammopathy (of renal significance), myeloma or lymphoma, the presence of C3GP in this population should prompt hematologic evaluation.

1608 Quantitative Assessment of Density of Deposits in C3 Glomerulopathies

Mark Lusco, Agnes B Fogo. Vanderbilt University Medical Center, Nashville, TN.
Background: C3 glomerulopathy (C3GP) includes a range of diseases from C3 glomerulonephritis (C3GN) to dense deposit disease (DDD), all with C3 dominant deposits and an etiology of alternative complement pathway dysregulation. C3GN is distinguished from DDD by location and perceived density of deposits on electron microscopy (EM). In some cases, intermediate deposit density causes difficulty in distinguishing these entities. We quantitatively assessed the density of C3 deposits to objectively characterize the spectrum of deposits in C3 glomerulopathy.
Design: We identified all renal biopsies at Vanderbilt University from January 2011-July 2015 with diagnosis of DDD or deposits with at least 2+ greater intensity for C3 than other complement or immunoglobulin by immunofluorescence (IF). Only biopsies with distinct glomerular deposits by IF with corresponding deposits on EM were included. Assessment of density (black content) in deposits, red blood cells (RBC) and glomerular basement membranes (GBM) was performed using Adobe Photoshop from 8-bit grayscale digital photographs or scanned prints. Within the same photograph, deposits, uninvolved GBM and RBC were included to ensure equal photographic exposure. The most frequent type, densest and most diagnosis-defining deposits were assessed. Density was determined by normalizing the black content on a scale of 0-100 based on the black content of uninvolved GBM (0) and RBC (100), thus, allowing comparison of density scores in different images and cases. In addition, 9 usual type immune complex glomerulonephritis (UTICGN) cases were assessed.
Results: 61 cases of C3GP were identified, and 3 lacked EM images or grid availability and thus were excluded. DDD (n=7) had the highest normalized density score, mean 91 (range 71-100). 3 cases with a diagnosis that included features of DDD had a density score mean 76 (71-81). Proliferative GN or post-infectious GN with dominant C3 (n=24) had deposit density score mean 60 (range 25-100). All other C3 dominant deposit cases (n=24) had a similar density score mean 60 (range 25-100). UTICGN control cases overall had lower density score with mean 54 (range 21-100).
Conclusions: The measurement of deposit density decreases as expected from DDD to UTICGN. C3GN cases showed similar density to UTICGN. Cases with features suggestive of, but not diagnostic of DDD, were objectively confirmed to show intermediate density of deposits. Thus, the measurement of characteristic EM deposit density may be a helpful guideline for characterizing disease with C3 dominant deposits.

1609 Renal Allograft Biopsy CD3+ Cell Quantitation Algorithm Development for Rejection Assessment Utilizing Open Source Image Analysis Software

Andres Moon, Geoffrey Smith, Thomas E Rogers, Carla L Ellis, Alton B Farris. Emory University School of Medicine, Atlanta, GA.
Background: Renal allograft rejection diagnosis depends on assessment of parameters such as interstitial inflammation; however, studies have shown wide interobserver variability. Commercial cell counting algorithms are currently available, with data suggesting correlation between densities of CD3 staining with severity of T-cell mediated rejection. Image analysis and automated quantitative methods may prove potentially more reproducible; therefore, we devised customized methods of analysis and compared these with established commercial methods along with visual assessment.
Design: Renal allograft biopsies with varying degrees of rejection were retrieved (n = 30), and CD3 immunohistochemistry slides were scanned to obtain whole slide images (WSIs). Inflammation was quantitated in the WSIs using pathologist visual assessment, commercial algorithms (Aperio nuclear algorithm to give CD3/mm^2 and Aperio positive pixel count algorithm), and customized open source algorithms developed in ImageJ which involved thresholding/positive pixel counting (Calculated CD3/mm^2) and identification of pixels fulfilling "maxima" criteria for CD3 expression (Custom CD3/mm^2).
Results: CD3 quantitation algorithms correlated between each other and also with visual assessment in a statistically significant manner (Fig 1). Methods for assessing inflammation showed a progression through the grades of tubulointerstitial rejection, with statistically different results in borderline versus other rejection cases (Fig 2), in all but the custom CD3 count method.

Fig 1. Multivariate correlation between various methods shows statistically significant r values for each of the correlations.

	Calculated CD3 / mm^2	Custom CD3 / mm^2	Positivity = NPositive/NTotal	Aperio CD3/mm^2	Visual CD3%
Calculated CD3 / mm^2		0.72	0.97	0.91	0.90
Custom CD3 / mm^2	0.72		0.65	0.70	0.52
Positivity = NPositive/NTotal	0.97	0.65		0.91	0.91
Aperio CD3/mm^2	0.91	0.70	0.91		0.82
Visual CD3%	0.90	0.52	0.91	0.82	

Calculated CD3 / mm^2 is computed from CD3 area/total biopsy area.
For all correlation r values, P<0.0001 except for custom algorithm vs. visual where P=0.00035.

Fig 2. Correlation of CD3 Quantitation with Diagnosis

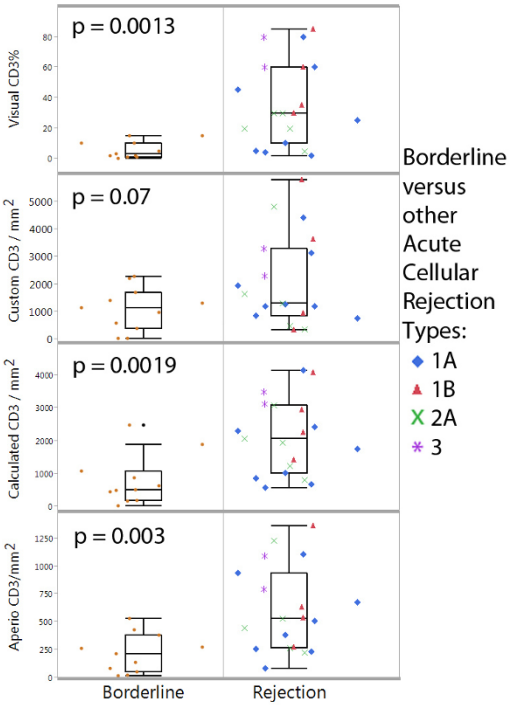

Conclusions: Assessment of CD3-stained slides using various open source image analysis algorithms shows correlation with established methods of CD3 quantitation. These analysis techniques are promising and highly customizable, providing a form of on-slide "flow cytometry" that may facilitate additional diagnostic accuracy in the assessment of patient material.

1610 Clinical Significance of the Pathological Evaluation of Non-Neoplastic Renal Tissue in Post-Radical Nephrectomy

Madeleine Moussa, Adiel Mamut, Gena Ibrahim, Patrick Luke, Fulan Cui, Neal Rowe, Manal Gabril. Western University, London, ON, Canada.

Background: Recent studies have demonstrated that the evaluation of non-neoplastic renal parenchymal tissue post partial nephrectomy may predict future renal function. We assessed the predictive role of non-neoplastic renal pathology in a cohort of patients with normal pre-operative renal function who underwent radical nephrectomy for a renal mass.

Design: All local patients with a normal contralateral kidney who underwent radical nephrectomy between April 2002 and May 2008 were identified. Patients with missing clinical data or pre-operative chronic kidney disease (CKD), defined as Glomerular Filtration Rate (GFR) <60mL/min/1.73m^2) were excluded. Pathology slides were re-reviewed by genitourinary pathologists (MM&MG) for presence of Glomerulosclerosis (GS), Interstitial Fibrosis (IF), Tubular atrophy (TA), and arterial narrowing (AN) which were correlated with pre and post-op renal function. Student's t test and logistic regression were used to assess statistical significance.

Results: Ninety seven patients met inclusion criteria and had tissue available for pathology review. GS, IF, TA and AN was present in 70%, 44%, 44% and 96% of patients, respectively. The presence of IF and TA was associated with relatively reduced renal function both pre-op and at 1 year. Patients with GS demonstrated significant decline in renal function at 1 year despite normal pre-operative renal function. Of the assessed clinical conditions, only hypertension and coronary artery disease were associated with poor post-op renal function on logistic Regression (p=0.04 and 0.04).

Table 1: Pathological Characteristics

Pathological Finding	N (%)	Mean 1 yr Creat. with path.	Mean 1 yr Creat. without path.	*p-value*
Glomerulosclerosis	68 (69%)	122.72	108.62	0.002*
Interstitial Fibrosis	43 (44%)	128.31	110.69	0.0003*
Tubular Atrophy	43 (44%)	128.31	110.69	0.0003*
Aterial Narrowing	91 (93%)	118.83	113.64	0. 055
≥ Pathologica Findings	75 (77%)	122.76	108.2	0.0016*

Conclusions: Evaluation of non-tumor renal tissue at the time of radical nephrectomy offers valuable predictive information regarding post-operative renal function. Significant pathological findings were common in our patient cohort. Our data suggest an ongoing role for pathological evaluation of non-neoplastic renal tissue in nephrectomy specimens. The overall impact of pathological evaluation needs to be evaluated in a larger cohort using multi-variable analysis.

1611 Leukocyte Chemotactic Factor 2 Amyloidosis (ALECT2) Is a Common Form of Renal Amyloidosis Among Egyptians

Samih Nasr, Wesam Ismail, Paul J Kurtin, Julie Vrana, Surendra Dasari, Christopher Larsen. Mayo Clinic, Rochester, MN; BeniSuef University, BeniSuef, Egypt; Nephropath, Little Rock, AR.

Background: Large case series of renal amyloidosis subtypes have recently been published in the U.S. and Europe showing AL amyloidosis to be the predominant subtype in this part of the world. However, the most common subtypes of renal amyloidosis throughout the rest of the world is unknown. We present here the first large case series detailing the subtypes of renal amyloidosis among Egyptians.

Design: The database from Pathlab institute in Cairo, Egypt was searched for cases of amyloidosis between 2012-2015. A total of 161 formalin fixed paraffin embedded kidney biopsies with amyloidosis were identified. These blocks were sent to Nephropath. A total of 116 blocks had sufficient tissue for amyloid typing. A Congo red stain was performed in all cases. Immunoperoxidase stains for AA as well as paraffin immunofluorescence for kappa and lambda were performed. Cases that were not able to be typed using these stains were sent to Mayo Clinic for typing by laser microdissection/mass spectroscopy

Results: AA amyloidosis was the most common type (n=56, 48%), followed by leukocyte chemotactic factor 2 amyloidosis (ALECT2) (n=36, 31%) then AL amyloidosis (n=23, 20%). The remaining case was a case of AFib amyloidosis. The pathologic findings in ALECT2 cases were similar to those previously described in U.S. case series, with cortical interstitial, glomerular, vascular, and medullary interstitial involvement in 100%, 84%, 76%, and 56%, respectively. Patient age at diagnosis for AA, ALECT2, and AL amyloidosis (mean 45, 59, 56 years, respectively) was younger than that reported in the U.S case series

Conclusions: ALECT2 amyloidosis, which was initially thought to affect mainly Hispanics in the U.S., appears to represent an important and likely underrecognized etiology of chronic kidney disease among Egyptians and probably in other ethnic groups around the world

1612 Glomerular Complement Factor C4d Deposits Are Structural Markers for Basement Membrane Duplication in Transplant Glomerulopathy and Thrombotic Microangiopathy

Volker Nickeleit, Harsharan Singh, Adil Gasim, Jamie S Chua. The University of North Carolina, Chapel Hill, NC; Leiden University Medical Center, Leiden, Netherlands.

Background: C4d along peritubular capillaries is a widely accepted marker for antibody mediated rejection in the renal allograft. However, the significance of C4d staining along glomerular capillary walls/basement membranes (GBM-C4d), especially if seen in isolation without peritubular capillary C4d staining, is not well defined.

Design: GBM-C4d staining was evaluated by immunofluorescence (IF) and immunohistochemistry (IHC) in 319 renal allograft biopsies and a control group of 35 native kidney specimens. GBM-C4d staining results were correlated with structural glomerular basement membrane abnormalities by light and electron microscopy (EM), morphologic signs of antibody mediated rejection and clinical data including the presence of donor specific antibodies.

Results: Peritubular capillary C4d deposition was associated with GBM-C4d in 97% by IF and 61% by IHC (p<0.001). Transplant glomerulopathy (n=52) significantly correlated with pseudolinear GBM-C4d (49/52, 94% positive by IF and 20/30, 67% by IHC, p<0.001). Immunogold labeling demonstrated GBM-C4d deposits along widened subendothelial layers with new lamina densa deposits. Staining intensity correlated with Banff cg scores of GBM duplications (rs=0.45, p<0.01) and the degree of subendothelial new densa multilaminations by EM. Early GBM duplications only seen by EM and not by light microscopy (n=30) were also associated with GBM-C4d. Stepwise exclusion and multivariate logistic regression showed significant correlations between architectural GBM changes with duplications and GBM-C4d staining corrected for peritubular capillary C4d deposits and antibody mediated rejection (p=0.001). Native control biopsies with chronic thrombotic microangiopathy showed GBM-C4d in 92% by IF, p<0.001, and 35% by IHC; no GBM-C4d present in minimal change disease.

Conclusions: The significance of GBM-C4d differs from C4d staining along peritubular capillaries. Pseudolinear GBM-C4d reflects two forms of injury: 1) thrombotic microangiopathy like structural changes with GBM duplications independent of a specific etiology/antibodies, or 2) active antibody mediated rejection characteristically accompanied by C4d along peritubular capillaries and spill-over GBM-C4d. The detection of strong, especially isolated pseudolinear GBM-C4d could optimize a diagnosis and potentially has therapeutic implications.

1613 IgA Dominant Post-Infectious Glomerulonephritis in the Pediatric Population

Paul Persad, Agnes Fogo. Vanderbilt, Nashville, TN.

Background: IgA dominant post-infectious glomerulonephritis (PIGN) occurs most often in older patients, with multiple co-morbidities and poor outcomes. Misdiagnosis of this condition as IgA nephropathy can be catastrophic; the former is treated by prompt antibiotic
therapy while the latter requires close follow up or immunosuppression. In children, IgA dominant PIGN is less well characterized and its prognosis is not known. We assessed frequency and prognosis of IgA dominant PIGN in children.

Design: We reviewed our archival biopsies over the past 10 years (2005-2015) for cases of glomerulonephritis with IgA dominance or codominance in patients less than

or equal to 18 years of age. Lupus nephritis, Henoch-Schonlein purpura nephritis and pauci-immune crescentic glomerulonephritis with IgA deposits were excluded. Demographic, clinical and pathologic were assessed.
Results: 1117 pediatric native kidney biopsies were examined, of which 72 cases revealed dominant or codominant IgA. Most of these, 63, were diagnosed as IgA nephropathy (IgAN), however, 9 cases (12.5%) were diagnosed as IgA dominant or co-dominance based on immunofluorescence findings, subepithelial hump-type deposits, prominent C3 and/or exudative lesions. IgA dominant PIGN patient ages ranged from 6 to 16 years, 7 Caucasian, 1 black and 1 Hispanic, 8 male and 1 female. Infections occurred in 6 cases (3 skin, 1 strep throat, 1 upper respiratory tract infection, and 1 pneumonitis). Initial serum creatinine ranged from 0.8 to 4.12 mg/dL. 4 patients presented with gross hematuria, 4 with microscopic hematuria and 1 had no hematuria. Two patients had proteinuria > 4 g/day. By light microscopy, all patients had endocapillary proliferation and/or crescent formation. 3 cases showed neutrophils in glomerular capillary loops. 3 cases showed 20-30% interstitial fibrosis. Compared to IgAN, all cases showed weaker immunofluorescence staining for IgG staining**.** 8 cases showed strong granular-chunky mesangial and capillary loop staining for C3. By electron microscopy, 6 cases revealed subepithelial "hump-like" deposits, 8 cases showed subendothelial deposits, and all cases contained mesangial deposits. All patients responded to therapy. 1 child developed cardiomyopathy and is on ACEI. 1 child developed liver failure several years later due to an unrelated illness. The remaining patients have regained normal kidney function and display no long-term renal sequelae.
Conclusions: IgA dominant PIGN is rare in the pediatric population. The overall good prognosis is in contrast to adult IgA dominant PIGN, which often leads to chronic kidney disease.

1614 ANA-Negative Renal-Limited Lupus Nephritis Is Associated with Poor Renal Outcomes

David Portnoy, Daphne Knicely, Warren K Bolton, James Cain, Helen Cathro. University of Virginia, Charlottesville, VA; The Johns Hopkins University, Baltimore, MD; Valley Nephrology Associates, Roanoke, VA.
Background: In 2012, the Systemic Lupus International Collaborating Clinics proposed biopsy-proven lupus nephritis (LN) plus positive ANA or ds DNA (DS) are sufficient for a diagnosis of SLE. We hypothesize that this definition is too narrow, and renal-limited lupus (RLL) may occur in serologically negative patients. ANA-negative lupus (ANL) was first described in 1976 by Koller in 5 patients with clinical SLE. No one has contrasted the renal outcomes in these patients with those of conventional seropositive LN patients, and it remains unclear whether these two groups are clinically distinct. To this end, we compare the entity of ANL and conventional LN with regards to pathology and renal outcome.
Design: This retrospective cohort study compares renal outcomes in 13 ANL patients vs. 44 control ANA-positive lupus (APL) patients. The definition of LN includes 'full house' staining and/or EM findings of LN. Other inclusionary criteria are ANA negativity and at least 6 mo. follow-up. Poor renal outcome is defined as doubling of creatinine, progression to dialysis or renal transplantation. Exclusionary criteria include HIV, Hepatitis B or C positivity. Control cases are time-matched with identical IF and EM criteria, but are ANA-positive.
Results: 7 ANL patients were ANA and DS negative. 11 ANL patients had 'full house' staining, none had tubular deposits, 6 had subepithelial, subendothelial and mesangial deposits, and none had TRIs. Two ANL and one control group case had positive PLA2R by IF. In the study group, 23% had poor renal outcomes vs. 27% in the control group, creating a relative risk of 0.85 (Fisher exact test p = 0.77).

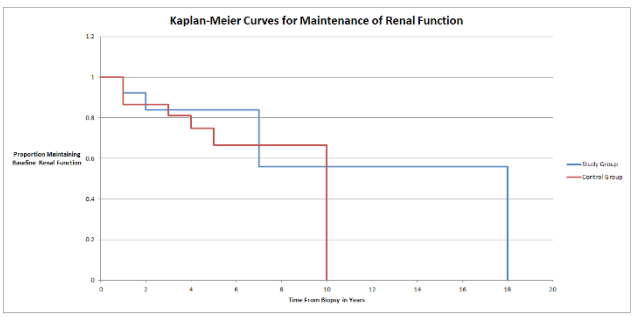

Conclusions: ANA is an unreliable screening test for SLE, and DS can also be negative in RLL. Pathologists should therefore have a lower threshold for diagnosing LN in patients with limited serology.
Rare cases of ANL and APL have IF PLA2R positivity; this may be less specific for primary membranous nephritis than previously believed.
This study suggests that renal outcomes in ANL are equivalent to those in conventional LN, supporting lupus-specific treatment of RLL.

1615 Hypoxia in Human Renal Disease, Always Suspected, but Not Usually Demonstrated: Analysis with Carbonic Anhydrase 9

Liza Quintana, Nika Aljinovic, Seymour Rosen. Beth Israel Deaconess Medical Center, Boston, MA; Boston Children's Hospital, Boston, MA.
Background: The conditions for demonstrating hypoxia in human renal disease are complicated, because oxygen utilization is more limited in the injured parenchyma (reduction of transport). The most valid marker of hypoxia is HIF 1 alpha, which degrades very quickly, but has been shown to be present in biopsies taken immediately after transplantation (J Am Soc Nephrol. 2007; 18(1):343-51). However, its closely allied gene target CA 9 persists for at least 96 hours after a normoxic environment is established (Biochim Biophys Acta. 2009; 1795(2):162-72).
Design: We present a series of 42 biopsies stained for CA 9: 4 groups were examined, 3 chosen because of a putative acute hypoxic element: delayed graft function (9); native AKI, commonly with an element of CKD (13); vasculopathy (10) including TMA (2), ANCA (6), malignant hypertension (1) and cryoglobulinemia (1). A fourth group represented chronic renal disease (10) and included IgA nephropathy, diabetes or chronic allograft nephropathy. Controls were nephrectomies and biopsies of failed transplants (3). Staining was graded on a 0-4+ scale; X +/- SE were calculated from positive cases.
Results: With near-total renal infarction, the renal capsule is viable and the subjacent renal parenchyma shows extensive up regulation of CA9, both in regenerating tubules and the capsule. Staining in the biopsies, when limited, was usually luminal. Increased staining ranged from luminal to complete tubular (proximal and/or distal) involvement. With more intense staining, podocytes, crescents and Bowman's capsular epithelium were also positive. Biopsies with pure delayed graft function were usually negative, except for two patients, one with a large compressing hematoma and another with recurrent FSGS. Native ATN cases (score 1.75 +/- 0.5) and vasculopathy cases (score 2.1 +/- 0.5) were 50% and 70% positive, respectively. The most intense staining was seen in the vasculopathy group, but the differences between the two groups were not significant. Chronic renal disease staining was essentially negative.
Conclusions: Hypoxia can be demonstrated in human renal disease, often when a vasculopathy is present. Uncomplicated delayed graft function and chronic kidney disease are generally negative. In AKI occurring in native kidneys, a hypoxic element can be shown and suggests ongoing active injury, in spite of diminished transport. This is the first study to provide evidence of hypoxic injury in a spectrum of renal diseases.

1616 The Pathology of 'Pure' T-cell Mediated Rejection in the Era of C4d Staining and Testing for Donor Specific Antibodies

Parmjeet Randhawa, Gang Huang, Simrath Randhawa, Gang Zeng, John Lunz, Xiaomu Zhao. The Thomas E. Starzl Transplant Institute, Pittsburgh, PA.
Background: Recent literature has stressed the prominent role of antibodies in acute and chronic graft loss. This study was designed to assess a growing perception that T-cell mediated rejection (TCMR) is no longer clinically relevant.
Design: 545 renal allograft recipients over a 3 year period were screened for biopsies satisfying the following criteria: (a) TCMR including borderline change (BL), (b) negative C4d stain, and, (c) absence of DSA at time of transplant, within 30d of the biopsy, and up to 4 measurements at later time points. Control renal allograft biopsies (n=14) were selected from the same time period as the study cases based on similar criteria, but with no evidence of TCMR, BL, antibody injury, C4d staining, infection, thrombotic microangiopathy, or glomerulonephritis.

Figure 1

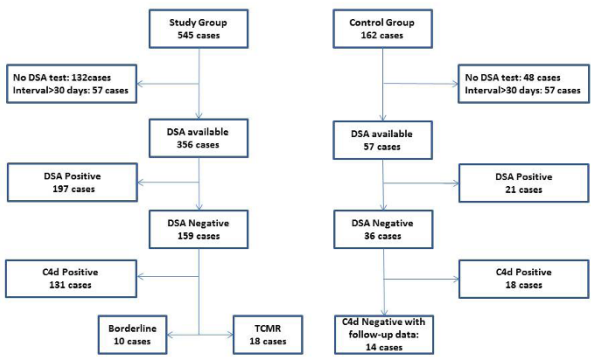

Results: These stringent requirements led to the identification of 18 cases of 'pure' TCMR and 10 BL cases. Interestingly, glomerulitis which is used as diagnostic criterion for ABMR was present in 1/10 BL biopsies (g=1) and 5/18 TCMR biopsies (g=1). Peritubular capillaritis was demonstrable in 1/10 BL biopsies (ptc score 1) and 8/18 TCMR biopsies (ptc scores 1 and 2 in 3 and 5 biopsies respectively). Chronic transplant glomerulopathy, another lesion said to be characteristic of chronic ABMR, was found in 1/10 BL biopsies (cg =1) and 3/18 TCMR biopsies (cg=1, 1, 3). Intimal arteritis (v=1) was found in 1/10 follow up TCMR biopsies. Serum creatinine showed complete short-term remission in 7/10 (70%) BL and 9/18 (50%) in TCMR patients 1m post-biopsy. Yet, both treated and untreated patients demonstrated further decline in graft function as assessed by serum creatinine and estimated GFR.
Conclusions: TCMR can cause significant deterioration of graft function in patients with TCMR in whom the dominant contribution of antibody mediated injury has been reasonably excluded Our data also reinforces existing literature showing that microvascular lesions do not have absolute specificity for a diagnosis of antibody mediated rejection.

1617 Renal Cell Carcinoma in Allograft Kidneys: Use of Short Tandem Repeat Analysis to Determine Donor Origin of Cancer

Adam Robin, Colin C Hansen, Lauren Parsons, Christopher Hartley, Eric Cohen, Alexander C Mackinnon. Medical College of Wisconsin, Milwaukee, WI.

Background: Post-transplant malignancy is an important complication of kidney transplantation. Renal cell cancers (RCC) in the native, failed kidneys are well-known, and are more common in kidney transplant and dialysis patients than the general population. RCC, while rare in transplanted kidneys, could arise from the recipient or the donor. This distinction has consequences for staging and therapy.

Design: At our institute 542 kidney transplants were performed between 2007 and 2011. In 6 cases, RCC developed in the allograft kidney. Archived formalin fixed paraffin embedded (FFPE) tissue was used as source tumor DNA, donor DNA was obtained from cancer-free regions of the kidney where available, host DNA was obtained from fresh leukocytes or microdisection of deparaffinized FFPE tissue sections. DNA was extracted and purified from these regions and from whole blood. Penta C (PC) and Penta D (PD) short tandem repeat loci were amplified using fluorescently-labeled PCR primers, resolved by capillary electrophoresis, and compared to determine donor origin of the RCC.

Results: Age of the kidney transplant recipients (KTR) at diagnosis was 32-63 years(yrs), mean: 47.5 yrs. Time lapse between transplantation and cancer diagnosis ranged from 9-30 yrs, mean: 17.75 yrs. Tumors were surgically removed by partial nephrectomy in 5 cases, and total nephrectomy in 1. Pathology reports confirmed RCC in all six cases. PC and PD alleles were robustly amplified in all samples. Each case had one or more informative PC or PD alleles. In cases with donor DNA samples, the PC and PD alleles from the cancer matched the uninvolved donor kidney PC and PD alleles. Furthermore, one or more host PC or PD alleles were absent from the cancer, showing that the cancer DNA is donor-derived. In one case, donor DNA was not available for analysis, so cancer and host alleles were compared. In this instance, none of the PD alleles matched in the two specimens, and each had a unique PC allele, indicating that the cancer is genetically distinct from the host.

Conclusions: Determination of tumor cell origin is significant for staging & treating RCC in renal allografts. Reduction of immunosuppression may cause cancer rejection for donor-derived cancers, but host-derived cancers may not respond. The PC and PD method is informative of sample identity over 99% of the time. Our data show that STR analysis is a simple strategy to determine donor versus recipient origin of cancers in kidney transplant patients.

1618 Loss of Glomerular Basement Membrane Staining for COL4A5 in Alport Syndrome Correlates with Age at Diagnosis and Severity of Ultrastructural Alterations

Samar Said, Mary E Fidler, Brooke McCann, Lynn D Cornell, Mariam Priya Alexander, Samih Nasr. Mayo Clinic, Rochester, MN.

Background: Alport syndrome (AS) is a hereditary disease of basement membranes. Most cases show X-linked inheritance due to mutations in the *COL4A5* gene; a minority are autosomal with mutations in *COL4A3* or *COL4A4*. The diagnosis of AS is based on the findings of glomerular basement membrane (GBM) splitting, basket weaving, and/or thinning. Immunofluorescence (IF) staining for COL4A5 on kidney can be used to confirm the diagnosis. It is unknown if there is a correlation between GBM staining for COL4A5 and severity of ultrastructural GBM alterations in AS.

Design: We performed IF using a mixture of FITC-conjugated and Texas-red-conjugated rat monoclonal antibodies against COL4A5 and COL4A2, respectively, on 41 renal biopsies with a pathologic diagnosis of AS. Normal staining of GBMs and tubular basement membranes (TBMs) for COL4A2 was observed in all cases. IF staining for COL4A5 was correlated with the clinical characteristics and biopsy findings. The severity of GBM ultrastructural alterations were graded as mild: <25%, moderate: 25-75%, and severe: >75% of glomerular loops showing GBM splitting/basket weaving (with/without thinning of other loops).

Results: Fourteen (34%) of the 41 cases showed loss of GBM staining for COL4A5, including 9 with concurrent loss of staining of Bowman's capsule (BC) and distal TBMs (consistent with X-linked AS, 3 were brothers) and 5 with preserved staining of BC and distal TBMs (consistent with autosomal AS). Compared with the 27 patients with preserved GBM staining for COL4A5, the 14 with loss of staining were younger (mean age at biopsy 14 vs. 27 yrs, p<0001), mostly males (86% vs. 41%, p=0.004), had higher incidence of hearing loss (58% vs. 16%, p=0.01), less global GS (5% vs. 18%, p=0.02) and more prominent GBM ultrastructural alterations (marked grade in 79% vs. 14%, p<0.001; mild in 0% vs. 59%). The degree of proteinuria or interstitial fibrosis and the presence of renal insufficiency, HTN, segmental sclerosis, foam cells, or family history of hematuria were not statistically different between the 2 groups.

Conclusions: Loss of GBM staining for COL4A5 correlates with younger age at diagnosis and more severe GBM ultrastructural alterations, likely reflecting larger genetic mutations in these patients. IF staining for COL4A5 is useful to predict the severity of genetic defects and to determine the mode of inheritance. In AS cases showing only mild/segmental GBM splitting, staining for COL4A5 is not helpful to confirm the diagnosis nor to distinguish AS from thin basement membrane nephropathy.

1619 Characterizing Glomerular Injury of Pediatric Kidneys Transplanted to Adult Recipients

Steven Salvatore, Meredith J Aull, Muthukumar Thangamani, Surya Seshan. Weill Cornell Medical College, New York, NY.

Background: Pediatric deceased donor kidneys have been used effectively in transplantation to standard weight adult recipients. Due to postulated hyperfiltration-induced glomerular injury, the recipients may manifest proteinuria in the post-transplant period with transplant (tx) biopsies revealing "pediatric donor glomerulopathy" (PDG). We aim to further characterize the spectrum of podocyte and glomerular injury.

Design: From 2006-2015, 52 kidney tx biopsies from 31 patients (of 85 total pediatric kidney recipients) were evaluated for LM, IF, and EM (27). Immunohistochemical (IHC) stains for glomerular epithelial antigens were performed on 29 biopsies. Clinicopathologic parameters including follow-up were analyzed.

Results: 31 patients' biopsies were studied, mean 353 days from tx (range 11-1820 d) for elevated creatinine, 0.7-21 mg/dL (M 3.9). 78% had proteinuria, 0-10g/24hr (M 2g). The donor ages were 2 mo to 6 yrs (M 24 mo) with weights 6.5-18.5kg (M 11.8kg). Donor to recipient weight ratio was 8.3-37% (M 20%). Biopsies showed PDG in 15/31, alone in 12 or with superimposed disease in 3. Other tx related diagnoses included rejection in 8 (3 ACR, 4 AMR, 1 mixed), acute tubular injury 4, CNI toxicity 3, BKV 1, TMA 1, recurrent MGN 1, and 1 protocol. Among PDG cases, 53% had fetal glomeruli, 4 with collapsing glomerulopathy. EM and IHC findings of glomerular injury listed in table.

CK positive epithelial cells	14 % (of cases)
Podocin lost	31%
WT1 lost	7%
Ki-67 positive epithelial cells	25%
Foot process effacement (>30%)	30%
Podocyte Vacuolization	88%
Podocyte Pseudocysts	56%
Microvillous transformation	56%
GBM lamellation (segmental/global)	37%
Endothelial injury/swelling	48%

Follow-up info was available on all cases for a mean 3.24 years (212 d to 7.9 yrs). Nine of 31 (29%) failed within mean 659 days (0-1193 d) , 21 had functioning grafts with Cr 0.95-4.4 and proteinuria 0-1.35 g at last follow-up, and 1 patient died with a functioning graft. Graft failures were from rejection (4/9), BKV (1), TMA (1), and only 3 had PDG. Overall, 13/21 pts had proteinuria and 12/21 had hematuria at last follow-up, 89% of patients had improvement in proteinuria.

Conclusions: Deceased donor pediatric kidneys are a viable option for increasing tx demands. While PDG associated podocyte and glomerular basement membrane injury may lead to proteinuria and hematuria in the post-tx setting, long term graft survival seems preserved. It is important to recognize this form of glomerular injury which may be amendable for therapeutic management.

1620 Patterns of Immune Complex Deposits in 70 Kidney Biopsies with Staphylococcus Infection Associated Glomerulonephritis

Anjali Satoskar, Sarah Suleiman, Jessica Hemminger, Sergey Brodsky, Gyongyi Nadasdy, Tibor Nadasdy. Ohio State University Wexner Medical Center, Columbus, OH.

Background: IgA-dominant immune complex deposits (along with C3) are considered key diagnostic features in Staphylococcus infection-associated glomerulonephritis (SAGN). However recent articles have reported that Staphylococcal endocarditis associated GN may show pauci-immune pattern and positive ANCA serology, causing diagnostic overlap with ANCA-associated GN. This has important implications in regards to choice of antibiotics or immunosuppressives. Immunosuppressive therapy is essential in ANCA GN, but can be detrimental in endocarditis-associated GN.

Design: We studied the immune complex pattern in 70 biopsies of SAGN (including endocarditis) diagnosed at our institution from January 2004 to June 2015, by immunofluorescence and ultrastructural examination. All 70 patients had culture proven Staphylococcal infection (table 1). Patients with infected abdominal mesh, infected ileal fistula, visceral abscesses, post-surgical infections, urinary tract infection and multiple simultaneous sites of infection were included in the "other" category in table 1.

Results:

	Endo-carditis n=12	Bacte-remia of unknown source n=9	Osteo-myelitis, septic arthritis n=15	Infected skin ulcers n=16	Pneu-monia n=6	Others n=12	Total n=70
Trace to absent IgA	3	3	6	3	2	4	21 (30%)
Trace to absent C3	0	1	4	3	0	4	12 (17%)
Trace to absent IgG	7	2	10	8	3	10	40 (57%)
C3 alone seen	2	1	3	2	1	2	11 (16%)
Pauci-immune pattern	0	1	4	1	0	3	9 (13%)
Pauci-immune pattern with crescents	0	0	2	0	0	3	4/9 (44%)
Total biopsies with crescents	5	2	6	2	4	5	24 (34%)
Biopsies with subepithelial humps	3	3	3	7	2	4	22 (31%)
ANCA positive	0	3	0	1	0	0	4/35 tested (11%)

Pauci-immune pattern was seen in 9/70 biopsies. Four of these 9 biopsies also showed focal crescents by histology. No vasculitic lesions were seen. Out of 35 patients tested for ANCA serology, 4 tested positive (3 pANCA, 1 cANCA), but these did not show crescents on biopsy. Subepithelial humps were seen in only 31% biopsies.

Conclusions: Weak to absent IgA does not preclude the diagnosis. C3 is usually present. Pauci-immune pattern of deposits and positive ANCA serology although infrequent, are potential diagnostic pitfalls in SAGN. Subepithelial humps are seen infrequently in SAGN.

1621 Glomerular Capillary Wall Staining with C4d Is Associated with Glomerular Proliferation in IgA Nephropathy

Umer Sheikh, Cynthia Cohen, Thomas E Rogers, Alton Farris, Hong Qu, Carla Ellis. Emory University Hospital and School of Medicine, Atlanta, GA; St. John Hospital and Medical Center, Detroit, MI.

Background: IgA nephropathy (IgAN) is one of the most common immune complex associated nephropathies worldwide. It may develop de novo or recur in an allograft. Recently, C4d immunohistochemistry has been shown to highlight immune complex deposits in a variety of glomerular diseases, including IgAN. This finding would be beneficial in cases where immunofluorescence studies are unavailable. Our study seeks to determine the ability of C4d immunohistochemistry to highlight IgA dominant immune complex deposition in native and allograft biopsies.

Design: A retrospective study from two institutions was performed. 24 cases (19 native and 5 allografts) from one and 33 native cases from the other (n=57) of IgAN diagnosed between the years of 2005 and 2012 were selected. All cases had a confirmed diagnosis of IgAN by immunofluorescence and electron microscopy. Paraffin-embedded tissue sections from all biopsies were then stained with the C4d antibody by each institutions immunohistochemical protocol. Cases from each institution were reviewed by the respective senior authors for the presence, intensity and location of glomerular staining by the C4d antibody.

Results: All native and allograft cases of IgAN from both institutions showed an absence of mesangial C4d immunoreactivity. Of the 33 native cases from one institution, segmental to global capillary wall staining was noted in all cases demonstrating glomerular crescents (8/8), p=0.0008. Focal capillary wall staining was also noted in 8 of the remaining 25 cases without glomerular crescents, and of those, 3/8 (36%) showed evidence of endocapillary proliferation. Control tissue from both institutions reacted appropriately.

Conclusions: Our results support recent findings that C4d can be a positive marker in immune complex mediated glomerulonephritis, specifically those cases with intra- or extracapillary cellular proliferation. Crescent formation is known to be associated with injury to/rupture of glomerular basement membranes and as such, the segmental to global capillary wall staining identified is likely associated with entrapment of the complement fragment along injured capillary walls. That no mesangial staining with C4d (to correspond with electron dense deposition) was noted suggests that C4d may act more as a responder to vascular injury (similar to that seen in antibody mediated allograft rejection) rather than a primary component of IgA predominant antigen-antibody complexes.

1622 Relationship Between Glomerular Macrophage Numbers and the Oxford Classification of IgA Nephropathy

Maria Fernanda Soares, Clare MacEwen, Aron Chakera, Shuba S Bellur, Ian SD Roberts. Federal University of Parana, Curitiba, Parana, Brazil; Oxford University Hospitals NHS Trust, Oxford, Oxon, United Kingdom; University of Western Australia, Perth, Western Australia, Australia.

Background: Endocapillary hypercellularity (E score in the Oxford Classification) is predictive of renal function decline in IgA nephropathy (IgAN) patients who do not receive immunosuppressive therapy. Patients with E1 on initial biopsy have a better renal survival if treated with steroids. However, data from the VALIGA study indicates that E score is poorly reproducible, limiting its value in routine clinical practice. We hypothesise that endocapillary hypercellularity is a consequence of inflammatory cell infiltration and that glomerular macrophage count can be used as an alternative, and potentially more reproducible, measure of E score.

Design: Macrophages were counted in each glomerulus, using immunohistochemistry for CD68, in a series of 112 IgAN biopsies. Macrophage counts for every sample were correlated with the MEST criteria of the Oxford Classification, obtained from PAS-stained serial sections.

Results: The range for the number of macrophages per glomerulus was 0-39. There was a strong correlation between median macrophage count and % glomeruli showing endocapillary hypercellularity with no correlation with the continuous M score, % segmental sclerosis and % tubular atrophy/interstitial fibrosis (table 1). Logistic regression analysis indicated that a maximum number of macrophages per glomerulus of 6 as the best cut off for distinguishing E0 from E1 (sensitivity 94.1%, specificity 68.1%, cut off 5.5, AUC: 0.885). 95% of biopsies designated E0 had a maximum glomerular macrophage count of ≤6. 83% of biopsies designated E1 had a maximum glomerular macrophage count of >6. This model showed no correlation between maximum glomerular macrophage count and other variables of the Oxford Classification.

Table 1. Correlation of median glomerular macrophage count with continuous MEST variables (*Pearson product-moment correlation coefficient) and linear regression r^2.

	Median Macrophage Count		
	r*	p	r^2
M continuous	0.107	0.264	0.012
E continuous	0.672	<0.00001	0.452
S continuous	0.102	0.288	0.010
T continuous	0.134	0.161	0.018

Conclusions: We conclude that endocapillary hypercellularity in IgAN is largely a product of glomerular macrophage infiltration and that maximum glomerular macrophage number in CD68-stained sections is an alternative to subjective E score.

1623 Accelerated Mesangial Repair by Mesenchymal Stem Cells (MSCs) Incubated with "Cocktail" of Trophic / Differentiation Factors

Jiamin Teng, Chun Zeng, Elba A Turbat-Herrera, Guillermo A Herrera. LSUHSC-Shreveport, Shreveport, LA.

Background: Using mesenchymal stem cells (MSCs) to repair the injured mesangium is a rather novel concept. Previous observations from our laboratory have shown that MSCs migrate to the damaged mesangial areas and phagocytose apoptotic mesangial cells (MCs), debris and excess matrix to repair the injured mesangium. The present study aimed at finding factors to accelerate the repair process and to figure out the mechanisms involved.

Design: Mesangial cells (MCs) were cultured as a single layer in 96-well plates (2D) and on Matrigel (3 and 6D). MCs after becoming confluent were made quiescent for 48 hours. Then, they were incubated with glomerulopathic light chains (GLCs) (10 ug/ml) purified from the urine of patients with renal biopsy-proven light chain-related amyloidosis (AL-Am) (n=3) and light chain deposition disease (LCDD) (n=3) for 4 days and subsequently labeled MSCs were added. TGF-β, PDFG-β, retinoic-acid and curcumin were added in the medium in different concentrations and timeframes to observe whether the repair process was altered. Samples were collected 10 days after the introduction of the MSCs (day 14) and processed for light and transmission electron microscopy. In addition, sequential photos were taken with the aid of the 6D Life Cell Imaging System.

Results: MCs revealed evidence of direct damage by the GLCs including apoptosis with apoptotic bodies released and formation of amyloid or accumulation of matrix, depending on the LC used. MSCs identified and migrated to areas where damage was present. When MSCs became activated they acquired a "macrophage" phenotype. They then became active in phagocytosing cell debris, apoptotic bodies and damaged extracellular matrix. After performing this function, they proceeded to differentiate into mature MCs. Curcumin enhanced the migration of MSCs to the damaged sites and stimulated the apoptotic process. PDFG-β acted as a proliferative factor for the residual MCs and MSCs while TGF-β increased new matrix deposition. Retinoic-acid enhanced differentiation of MSCs into MCs.

Conclusions: MSCs actively clean the injured mesangium by phagocytozing apoptotic cells and other material. They do so by transforming into a macrophage phenotype. Once the cleaning process is completed, they differentiate into MCs acquiring their characteristic smooth muscle morphology and functional properties. The process could be regulated and accelerated by growth and differentiating factors making MSCs more effective in mesangial repair, remodeling and regeneration .

1624 PLA2R+ Membranous Nephropathy Has Greater C3 Deposition Than Non-Lupus PLA2R- Membranous Nephropathy

Mirna Toukatly, Behzad Najafian. University of Washington, Seattle, WA.

Background: Membranous nephropathy (MN) is the leading cause of nephrotic range proteinuria in none-diabetic adults with 40-50% of untreated patients progressing to end-stage renal disease. Activation of complement pathway is the best known mechanism of podocyte injury in MN. IgG4 anti-PLA2R is the main antibody involved in primary (1°) MN, while IgG4 does not activate classical complement pathway. In contrast, secondary (2°) MN are typically PLA2R- with deposition of other IgG subtypes that activate classical complement pathway. We examined if C3 deposition is different between PLA2R+ and PLA2R- non-lupus MN.

Design: Data from consecutive 54 (M/F=1.3/1) cases of 1° MN (PLA2R+) and 44 (M/F=1.4/1) cases of non-lupus 2° MN (PLA2R-) were compared for the immunofluorescence (IF) pattern and intensity of IgG, IgA, IgM, C3 and C1q (0-4+ scale), percentages of global (% GS) and segmental glomerulosclerosis (% SS).

Results: There was no difference in age or serum creatinine between the groups. Biopsies with 1° vs. 2° MN showed greater intensity for IgG (3.7 ± 0.7 vs. 2.9 ± 0.9, p=0.000001) and C3 (1.0 ± 1.0 vs. 0.68 ± 0.89, p=0.048). 1° MN had a trend towards any C3 staining (42.9% vs. 29.6%, p=0.08). Moreover, the intensities of IgG and C3 correlated in 1° MN (r=0.30, p<0.05), but not in 2° MN. Biopsies with 1° MN showed greater % GS (11±20%) than those with 2° MN (13±15%, p<0.025). %GS directly correlated with age and serum creatinine in both 1° and 2° MN, but %SS correlated with serum creatinine only in 1° MN. 1° and 2° MN were not different in IgA, IgM, or C1q staining intensities, or % SS.

Conclusions: While 1° MN is typically associated with deposition of IgG4 which does not activate classical complement pathway, we found more C3 deposition in 1° MN vs. 2° MN. Our findings are supportive of recent studies indicative of activation of complement system through pathways other than classical (i.e. mannose binding lectin pathway) in 1° MN.

1625 Vinyl Carbamate Induces Membranoproliferative Glomerulonephritis in an In-Bred Murine Bioassay Model

Neha Varshney, Paula M Kramer, William T Gunning. University of Toledo, Toledo, OH.

Background: Cancer remains a major cause of morbidity and mortality. The strain A/J mouse has been utilized for decades as a sensitive lung tumor bioassay model to determine relative carcinogenicity of various chemicals. This mouse is sensitive to carcinogens and if exposed, can develop multiple lung tumors that can be enumerated to determine the relative carcinogenicity of a specific chemical. More recently, the strain has been used to determine the efficacy of putative chemoprevention agents to inhibit lung tumor development. Several chemical carcinogens have been used in these chemoprevention bioassays including benzo(a)pyrene, methylnitrosourea and ethyl carbamate (EC, urethane) for eg. A metabolite of EC is vinyl carbamate (VC), also a potent carcinogen. Vinyl carbamate occurs naturally in fermented foods and alcoholic beverages; it has been reported to induce human cancers in lung, skin, liver, mammary gland and lymphoid tissues. We report unexpected findings from a chemopreventive bioassay using VC to induce lung tumors.

Design: The experimental design of a bioassay to investigate the efficacy of potential chemopreventive agents utilized 5-6 weeks old female strain A/J mice. They were administered VC at 60 mg/kg, a dose established in the literature, via intraperitoneal injection to induce lung tumors. The experiment utilized multiple groups of animals with 47 vehicle control animals and 279 mice given the carcinogen. Mice were scheduled to be sacrificed at various time points beginning at 5 weeks through 24 weeks post carcinogen treatment to evaluate lung tumor multiplicity.

Results: At 5 weeks post treatment, mice had evidence of a moribund state; these mice were killed and total necropsy was performed. At 12 weeks post treatment, a total of 97 of the 279 treated mice (37.8%) had died or were killed. Necropsies of mice that were moribund had been injected with 60 mg/kg VC were found to have developed membranoproliferative glomerulonephritis (MPGN). Control animals showed no evidence of renal disease.

Conclusions: Although VC has been successfully used to induce mouse lung tumors with no reported side effects, we found profound and unexpected renal disease associated with the chemical. The etiology of MPGN has been associated with immune complex–mediated conditions, autoimmune diseases, chronic infections (Hep C), chronic microangiopathies, and malignant neoplasms like lymphoma,carcinoma etc. As VC is known to occur naturally in human diets, could exposure in some foods be a risk factor for MPGN in humans? This model may be fruitful for potential research studies of MPGN.

1626 Validation of an Automated Platform to Assess the Total Inflammatory Load in Kidney Transplant Biopsies Using CD45 Immunohistochemistry and Computer-Assisted Quantitative Image Analysis

Vighnesh Walavalkar, Sarah Bowman, Hale Kirimlioglu, Laura Laszik, Brad Barrows, Jarish Cohen, Daniel E Roberts, Zoltan Laszik. UC San Francisco, San Francisco, CA.

Background: Total inflammatory load (TIL) is an important variable for the pathologic assessment of transplant kidney biopsies (TxBx). However, estimation of TIL using conventional light microscopy is suboptimal. The objective of our study was to validate a CD45 immunohistochemical (IHC) assay combined with whole slide imaging (WSI) and computer-assisted quantitative image analysis (QIA) with the future goal of standardizing the estimation of TIL in TxBx.

Design: Transplant kidney biopsies with normal morphology (NL), borderline change (BL), and acute cellular rejection (ACR) were enrolled into the study. From each case, 2 serially cut 3um-thick sections were stained for CD45 on a Leica Bond RX platform using standardized IHC on consecutive days. Whole slide digital images generated on an Aperio platform were analyzed using Definiens Tissue Studio 4.1 software for CD45 IHC signal. Linear regression analysis was used to assess the repeatability of the assay performed on separate days.

Results: The quality of two sections was suboptimal and therefore only 41 cases were analyzed [NL (n=14 pairs); BL (n=16 pairs) and ACR (n=11 pairs)]. Linear regression analysis showed 95% confidence intervals for separate day processing with a slope of 0.991986 (y-intercept = 0.017405, and R^2= 0.9951).

Conclusions: The results demonstrate high degree of repeatability for the CD45 IHC with the aid of computer-assisted image analysis in TxBx. The assay with standardized staining, scanning and image analysis protocols can be used in future studies to assess the utility of precise TIL measurements in TxBx.

1627 Molecular Diagnostics for Glomerulonephritis in Routine Formalin-Fixed Paraffin-Embedded Native Kidney Biopsies

Kristalee Watson, Benjamin Adam, Neesh Pannu, Michael Mengel. University of Alberta, Edmonton, AB, Canada.

Background: Molecular diagnostics have the potential to improve the classification and activity staging of native kidney diseases. The NanoString nCounter gene expression platform is unique in its ability to use formalin-fixed paraffin-embedded (FFPE) tissue samples, and represents a potential method for routine molecular diagnostics in renal pathology. We aimed to utilize this platform to assess the validity of gene expression quantification in crescentic glomerulonephritis (GN) in FFPE native kidney biopsies.

Design: A literature-derived gene set for glomerular and nephron injury was generated including 54 transcripts related to podocytes, endothelial cells, M2 macrophages, NK cells, and inflammation pathways. RNA was isolated from 332 FFPE native kidney biopsies, including 225 with crescentic GN, 81 with non-crescentic proliferative immune complex GN (e.g. IgA, post-infectious, SLE, membranous), and 26 with non-crescentic non-proliferative glomerular diseases (e.g. minimal change, hypertension, diabetes). Gene set expression was quantified with NanoString and correlated with histology.

Results: Gene set expression was higher in cases with crescentic GN than non-crescentic proliferative immune complex GN (p<0.001) and non-crescentic non-proliferative glomerular diseases (p<0.001). There were no statistically significant differences in gene set expression between the two non-crescentic groups (p=0.125) nor among the eight entities with crescentic GN (p=0.15-0.96). Gene set expression correlated with the degree of interstitial fibrosis and tubular atrophy (r=0.34, p=0.001). Genes associated with nephron injury correlated with the proportion of crescentic glomeruli (r=0.39, p<0.001), including cellular (r=0.24, p=0.002), fibrocellular (r=0.31, p<0.001), and fibrous (r=0.18, p=0.02) crescents.

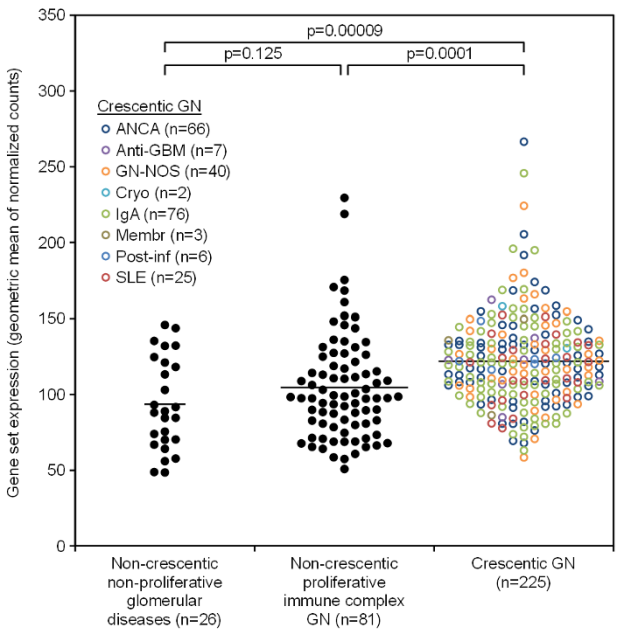

Conclusions: Our results demonstrate the feasibility of robust multiplexed gene expression quantification from archival FFPE native kidney biopsies. Measurement of a literature-derived gene set with the NanoString platform provides additional diagnostic information that may allow for more precise classification and risk stratification of patients with crescentic glomerulonephritis.

1628 Immunotherapy Mitigates Racial Disparities in Lupus Nephritis Outcomes

Parker Wilson, Michael Kashgarian, Gilbert Moeckel. Yale University School of Medicine, New Haven, CT.

Background: Lupus nephritis (LN) is a major contributor to morbidity and mortality in systemic lupus erythematosus. African Americans (AA) have a higher risk for progression to ESRD, which has been attributed to socioeconomic status, disease severity, and genetic differences.

Design: 301 consecutive cases of biopsy-proven LN were retrospectively identified at our institution from 1998 - 2014 and categorized by ISN/RPS criteria. Patients biopsied

prior to 1998 were excluded. Survival was defined as the time from initial biopsy to eGFR < 15mL/min, renal replacement therapy, or death. Immunotherapy (IMT) was defined as any treatment with cyclophosphamide, azathioprine, mycophenolate mofetil, or rituximab.

Results: 211 patients had follow-up data (AA=80, W=106, Asian=7, NS=18). African Americans (AA) had a larger proportion of class V LN at presentation (27% vs. 16%, p=0.04). Age, BP, BMI, Diabetes, SCr, 24h protein, C3, C4, ANA, and anti-dsDNA Ab positivity were similar between AA and white patients. Results are mean (SD). Baseline characteristics of other groups were not different (not shown). Overall, AA had shorter survival compared to white patients [HR 1.7, 95% CI: 1.0 to 2.8, p=0.042]. Similarly, AA without IMT had shorter survival compared to white patients without IMT [HR 2.2, 95% CI: 1.0 to 4.8, p=0.046]. However, AA with IMT did not have different survival compared to white patients with IMT [HR 1.1, 95% CI: 0.5 to 1.1 , p=0.71].

Conclusions: Immunotherapy reduces the risk for progression to ESRD and closes the gap in racial disparities between African American and white patients.

*=Baseline #=Follow-up	Black	White
*No. Patients (%Female)	94 (84)	132 (80)
*Age	35.6 (14)	32.9 (14)
*SCr	1.4 (1.2)	1.3 (0.9)
*24h Protein	3.9 (2.5)	2.9 (2.4)
*ISN/RPS Class II	15	20
III/IV	49	82
III/IV+V	3	8
V	26	22
VI	1	0
#No. Patients with Follow-up	80	106
#Median Follow-up (y)	5.2	7.0
#Median Survival (y)	12.1	16.5
#ESRD or RRT	14	22
#Death	15	9
#Immunotherapy	58%	66%

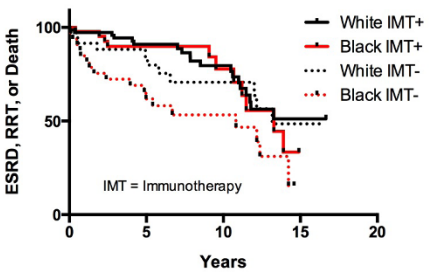

Liver

1629 Clinical and Pathologic Features of Nutritional and Herbal Supplements Induced Liver Injury

Gabriel Acosta-Gonzalez, Mark Ettel, Ogechukwu Eze, Shweta Gera, Cristina H Hajdu, James S Park, Samuel Sigal, Ruliang Xu. NYU Langone Medical Center, New York, NY.

Background: Certain nutritional and herbal supplements may have potential hepatotoxic effects. With increasing use of these supplements in the general population, supplements-induced liver injury (SILI) has become a common problem clinically. However, there is not much data about the clinical and pathologic features of SILI, and pathological characteristics of SILI have not been defined.

Design: All liver biopsy cases with diagnoses of hepatitis or liver injury were reviewed from our pathology database from 2014-2015. The cases of SILI were confirmed by pathological and clinical correlation. Pre-biopsy liver function tests (LFTs) were collected from the electronic medical record system. The H&E and Trichrome stain slides were re-assessed for pathologic changes. The morphologic patterns of liver injury, including bile duct injury, portal inflammation, interface hepatitis, lobular inflammation, fibrosis, presence of granulomas, and plasma cell and eosinophil infiltrates were recorded and analyzed.

Results: Total 17 cases of SILI were identified from 323 liver biopsy cases of hepatitis and liver injury. Two of 17 patients with SILI developed acute fulminant hepatic failure and succumbed to the illness. The hepatotoxic nutritional/herbal supplements identified included boswellic acid, carnosyn beta-alanine, whey protein, maca extract, rhodiola, holy basil, creatine, and some unspecified tea and anti-itching supplements. Histologically, the major pattern of liver injury was combined bile duct damage and hepatitis, and the majority of cases showed significant cholestasis. Fibrosis ranged from mild portal fibrosis to cirrhosis. No granulomas were identified. Plasma cells were rare to minimal in all cases, while eosinophils ranged from none up to 12 per high power field. Serologically, the mean values of alanine transaminase, aspartate transaminase, alkaline phosphatase, and total bilirubin were 625 U/L, 447 U/L, 241 U/L, and 12 mg/d, respectively.

Conclusions: Nutritional and herbal supplements have become a common cause of drug induced liver injury that may be under recognized. Histologically, the pattern of SILI in this study is the combination of bile duct and hepatocytic damage, ranging from mild disease to fulminant hepatitis. Significant elevation of LFTs, in combination with mixed pattern of liver injury should trigger the consideration of SILI.

1630 Distinctive Morphologic Pattern and In Situ Hybridization for Albumin Distinguishes Intrahepatic Cholangiocarcinoma from Metastatic Adenocarcinoma

Tanupriya Agrawal, Osman Yilmaz, Ricard Masia, Lipika Goyal, Andrew Zhu, Vikram Deshpande. Tufts Medical Center, Boston, MA; Massachusetts General Hospital, Boston, MA.

Background: The distinction of intrahepatic cholangiocarcinoma (IHCC) from metastatic adenocarcinoma is challenging and entails an extensive evaluation to exclude metastatic carcinoma. Albumin, detected on an in situ hybridization platform, is a robust means of distinguishing IHCC from metastatic adenocarcinoma. More recently, IDH1/2 mutations, in the context of biliary tract cancers , have been shown to be highly specific for IHCC. We evaluated the morphologic spectrum of IHCC, in conjunction with albumin expression and IDH mutation status, with the goal of distinguishing IHCC from metastatic adenocarcinoma.

Design: We evaluated 101 cases of IHCC. Histologic patterns evaluated included: anastomosing, tubular, pancreatic, undifferentiated, large duct and cribriform. Targeted sequencing for IDH1/2 mutations and in situ hybridization for albumin was performed in selected cases.

Results: The dominant histologic pattern was anastomosing (41% of cases and as a minor pattern in an additional 24 cases (24%), characterized by angulated anastomosing glands lined by low cuboidal epithelium. Other, albeit less characteristic dominant patterns included tubular (37%); nested (16%), mimicking a neuroendocrine tumor; undifferentiated (10%); pancreatic (6%), mimicking pancreatic ductal adenocarcinoma; large duct (2%); and cribriform (1%). All tumors tested for albumin (60 cases) were positive. There was no correlation between the histologic pattern and strength of the albumin signal with the exception of undifferentiated tumors, 50% of which showed reactivity only seen at 40x objective. 6 of 18 (33%) cases revealed IDH1/2 mutations. A survey of 655 adenocarcinomas, including primary tumors from the gastrointestinal tract, pancreas, lung, breast and ovary, identified only 2 tumors with an anastomosing pattern, both lesions arose in the pancreas.

Conclusions: The presence of an anastomosing growth pattern is highly suggestive of IHCC, noted in 64% of cases. Intratumoral albumin supports a diagnosis of IHCC, and when seen in isolation could also differentiate IHCC from metastatic adenocarcinoma. The combination of an anastomosing histological pattern and albumin reactivity, with or without detection of IDH1/2 mutations, should allow for a definitive diagnosis of IHCC in the vast majority of cases.

1631 Diagnostic Accuracy of the Liver Imaging Reporting and Data System (LI-RADS) for Hepatic Nodules in Cirrhotic Patients: A 2 year Retrospective Analysis

Hana Albrecht, Richard Gilroy, Ryan Ash, Maura O'Neil. University of Kansas Medical Center, Kansas City, KS.

Background: LI-RADS was created in 2008 by the American College of Radiology to standardize terminology and reporting of CT and MRI for hepatocellular carcinoma (HCC). Imaging plays a critical role in detection, diagnosis, and staging of HCC. The purpuse of our study is to evaluate the diagnostic accuracy of LI-RADS for hepatic nodules in explanted livers.

Design: Between 8/3/2013-8/3/2015, all liver explants with a diagnosis of HCC were retrieved from the pathology electronic record system (CoPath). The histologic diagnosis for each nodule was correlated with the LI-RADS interpretation. For the benign lesions, the histologic diagnosis was documented if the nodule was sampled and the location correlated with that reported radiographically. For the HCCs, the tumor histologic grade, size, multiplicity, and treatment effect were studied.

Results: Final diagnoses of 143 nodules in 67 patients were correlated with the LI-RADS category.

	Histologic Diagnosis in Explant Specimen	
LI-RADS Category	Regenerative Nodule	Hepatocellular carcinoma
0		34 (24%)
1		
2		
3	4 (27%)	11 (73%)
4	1 (9%)	10 (91%)
5	6 (7%)	77 (93%)

11 regenerative nodules and 98 HCCs were documented. An additional 34 nodules of HCC (24% of total nodules) were identified by histology only and not seen on pre-transplant imaging. These nodules ranged in size from <0.1 cm to 4.0 cm. 64% of these nodules measured ≤1.0 cm. Larger nodules (3-4cm) were comprised of many small tumor nodules growing in a military-type pattern. Treatment effect of 73 nodules was correlated with the LI-RADS suspicion (low, moderate, or high) for residual HCC.

Suspicion of residual HCC by imaging	0% viable	1-49% viable	50-99% viable	100% viable
Low	12 (22%)	17 (32%)	18 (34%)	6 (11%)
Intermediate	1 (25%)		2 (50%)	1 (25%)
High	0	3 (19%)	4 (25%)	9 (56%)